

Date: April 1<sup>st</sup>, 1948. 36

M. A. P. VOLKENRODE

AVA MONOGRAPHS

GENERAL EDITOR: A. BETZ.

BEST AVAILABLE COPY

B BOUNDARY LAYER.

EDITOR: W. TOLMIEN.

4 EXPERIMENTS ON THE INFLUENCE ON BOUNDARY LAYERS.

4.1 MAINTAINING THE LAMINAR CONDITIONS BY MEANS OF THE  
SHAPE  
(LAMINAR PROFILES).

4.2 MAINTENANCE OF THE LAMINAR CONDITIONS BY SUCTION.

4.3 INFLUENCE OF SURFACE CONDITIONS ON THE TRANSITION  
POINT.

BY

H. HOLSTEIN.

LABORATORY

BEST AVAILABLE COPY



UNCLASSIFIED

(NASA-TM-79794) AVA MONOGRAPHS. B:  
BOUNDARY LAYER (National Advisory Committee  
for Aeronautics) 53 p

N78-78473

00/02 Unclass  
29359

M.A.P. Völkenrode Ref.: MAP - VG 305 - ... T

#### 4 Experiments on the Influence on Boundary Layers.

Though we should only discuss experimental papers in this chapter we could not but make some theoretical considerations, too, for, according to the special conditions under which this summary is given, it must first satisfy the requirement of completeness - contrary to a text-book for instance - irrespective of the state of perfection of the subject in question. It follows that this survey would only be a loose enumeration of facts if it were limited to the test results alone in cases where we dispose of incomplete or even few tests only. Here, the connection can only be found by means of theoretical considerations.

For the subject to be treated there results a division into three parts. The first two parts deal with the means applied in order to keep the flow laminar along the greatest possible part of the surface: the suitable choice of the shape of the body which led to the development of the so-called laminar profiles in the case of aerofoils, and on the other hand the removal of the boundary layer material near the wall by sucking off. The sensitivity of the laminar boundary layer to disturbances on the surface of the body will be discussed in the third section.

We need not discuss problems of experimental technique, since no special experimental methods were developed for measuring boundary layers. Boundary layers and transition points were measured in the well-known way by means of the total-pressure tube. The measurement of the boundary layer was often completely relinquished and the wake behind the body was measured instead. This measurement is simpler and yields the drag from which a conclusion on the approximate position of the transition point can be drawn.

##### 4.1 Maintaining the Laminar Conditions by means of the Shape (Laminar Profiles).

By H. Holstein.

##### 4.11 Survey and Limitation.

The aim of reducing the resistance of the aerofoil as far as possible has occupied aerodynamic profile research in recent years by the development of the so-called laminar profiles. These are profiles for which the region of the laminar boundary layer from the stagnation point of the transition point was extended to a greatest possibly part of the surface. We must not be surprised

that this new trend of development obtained its improvements with respect to resistance only with deteriorations of other important profile characteristics such as maximum lift and curve of moments, since the aerofoil already had been developed to a high degree. This is the case at least for the test results obtained so far. Moreover the unfavourable fact that only about 1/6 of the resistance saved acts as relative velocity increase will be the reason why no very great attention was paid to the development of laminar profiles in Germany. The systematic experimental investigation of the conditions of keeping the boundary layer of aerofoil profiles laminar, therefore, is still in its first stage whereas the experimental investigation of the transition and of its cause was not made at all. The following statements, therefore, will be limited to indicate the laws of transition for laminar profiles by means of the available test results. As to the study of the properties of the laminar profiles in view of the  $C_{L_{max}}$ -behaviour, for example, with and without lift-increasing means, see monograph E 6.1.

#### 4.12 Influence of the Position of the Transition Point on the Resistance.

##### 4.121 The Possible Savings of Resistance (Theoretical).

Before treating the test results on laminar profiles let us give a small theoretical discussion of the flat plate in parallel flow, since it gives a good survey on the possible savings of resistance obtained by keeping the laminar conditions to a greater extent. The Reynolds numbers  $R$  or  $R_{crit.}$  respectively, are defined by means of the velocity of the incident flow and the chord of the plate or the laminar running length up to the transition point. Moreover  $C_{D \text{ lam.}}$  is the drag coefficient of a plate with laminar flow as far as its trailing edge and  $C_{D \text{ lam.-turb.}}$  is the drag coefficient of a flat plate which has its transition point at the point corresponding to  $R_{crit.}$  Now we assume that it would be possible by some measures to increase the critical Reynolds number of the plate from  $R_{crit.}$  to  $R$ , in other words to displace the transition point from its original position to the trailing edge of the plate. The relative saving of resistance obtained by this backward displacement is then obviously given by

$$1 - \frac{C_{D \text{ lam.}}}{C_{D \text{ lam.-turb.}}}$$

It is easily taken from Fig.1 for the values  $R/R_{crit.}$  between 1 and 100. Hence the savings increase with increasing abscissa; i.e. it is greater, the greater the part of the plate-chord covered by the displacement of the transition point. The fact that the savings also increase for a fixed value of the abscissa with increasing  $R_{crit.}$  is due to the stronger decrease of the laminar drag coefficient with increasing  $R$ -number than that of the turbulent drag, and hence the relative differences between both, and with them the positive savings, increase with increasing  $R$ . With the relatively small critical Reynolds number of  $0.5 \times 10^6$ , for instance, we save more than 50 per cent. of the resistance if the transition point is displaced from the centre of the plate to the trailing edge.

#### 4.122 Pressure Distribution and Position of the Transition Point. Disposition of the Test Results.

Whereas the transition point of the flat plate can be displaced backwards by means of a perfection of the surface only, we can obtain this in the case of the aerofoil by a suitable variation of the pressure distribution, too. This means was already recommended by the well-known considerations of stability (compare B 3) on profiles with laminar boundary layers: The laminar boundary layer is less sensitive to disturbances during the pressure drop than during the pressure rise. Therefore the pressure minima were displaced backwards on both sides of the profile as far as possible in order to obtain the longest possibly way of the laminar flow. Fig.2 shows the pressure distribution of a usual symmetrical NACA-profile (NACA 0010) [7] 10 per cent. in thickness as compared with that of a symmetrical laminar profile [4] of equal thickness. The latter has a greater backward position of thickness and a smaller nose radius. Due to these alterations the pressure minimum is displaced backwards from about 5 per cent. to about 60 per cent. of the chord.

Based on the fact that mainly the pressure distribution will affect the position of the transition point, the laminar profiles were developed in different ways:

- 1) The pressure distribution was given and the corresponding profile shape was calculated after one of the well-known methods [2].
- 2) The special family of J o u k o w s k i - profiles was taken as a basis for calculating suitable pressure distributions by varying the profile parameters [3, 7, 23].

3) Bisymmetrical contours such as circular arc bi-angle [1, 5] or ellipse [2, 10] were taken as a basis. They are known to have the pressure minimum at 50 per cent. of the chord.

4) The class of the NACA-profiles was systematically extended to shapes with greater backward positions of maximum thickness and smaller nose radii [5, 16].

5) The laminar profiles which had become known from abroad were tested and were taken in some cases as a basis for further development. These were the Japanese profile Tokio LB 24 [7], the profile NACA 27215 [7], the Mustang-profile [8, 9, 11, 18, 21, 22, 26], and the so-called "Russian laminar profile" [15, 17, 19, 20, 23, 25].

#### 4.123 Test Results, especially for Symmetrical Profiles in Symmetrical Flow.

For the R-numbers of few millions at which these profiles were first investigated the measurements generally gave the wanted success with respect to the decrease of resistance. The transition points mostly lay in these cases at 70 to 80 per cent. of the profile chord and correspondingly the drag coefficient  $C_D$  decreased to about half the values of the usual profile.

This decrease of  $C_D$  continued even when extreme profile shapes were chosen e.g. with a thickness of 15 per cent., a backward position of thickness of 65 per cent., and as angle of the trailing edge of  $40^\circ$  [7]. This will first be surprising on account of the turbulent boundary layer, which is probably very thick at the trailing edge. We realize, however, that the turbulent boundary layer will quickly increase at the transition point due to the great pressure rise which in its turn decreases the skin friction. Since the relatively great turbulent skin friction shortly after the transition generally gives rise to the main portion of the resistance, a reduction of these stresses due to considerable pressure rise may even have a favourable effect. Such an effect was actually stated by means of measurements on profile shapes which were especially designed for this purpose [12, 13].

Since the pressure distribution is the essential property which - for given R-number and technically unobjectionable profile surface - determines the behaviour of the laminar boundary layer, every kind of representation of the laminar properties by

means of unspecified profile parameters (for instance thickness, backward position of thickness, camber etc.) is incomplete, for they will at best determine the pressure distribution of the special profile family in question. Let us mention for explanation that the contour of a "profile family" is represented by one formula in which a more or less great number of parameters remains free. Nevertheless we depend on such a representation if we want to gain a survey on the aerodynamic properties of the laminar profiles. Moreover if not the absolute measuring values at least their variations with the profile parameters can be extended to other profile families. As we shall see later on, we can restrict ourselves to symmetrical profiles without an essential limitation of the general validity. Only three profile parameters decisive for the laminar conditions remain in this case.

These are:

$$t/l, x_t/l, \varphi_N \cdot l/t^2$$

where  $l$  is thickness,  $x_t$  its position, and  $\varphi_N$  the nose radius. The last mentioned profile parameter is called the nose coefficient and has been formed in such a way as to obtain always the same value for profiles of the same profile family with the same backward position of thickness. For the ellipse, for instance, its value is 0.5, whereas for NACA-profiles it is 1.1.

Apart from unusual cases (sudden curvature change the profile contour! compare section 4.3) the drag coefficient for symmetrical profiles is smallest for symmetrical incident flow. Here the sum of the laminar ways on the upper and lower sides has its maximum value. Hence the test results of a series of symmetrical profiles in symmetrical flow and with constant R-number can depend on the three above-mentioned parameters only. The only measuring series which is great enough for such a consideration was made with profiles of enlarged NACA-systematics [3]. The measured drag coefficients are plotted against the backward position of thickness, and measuring points associated to profiles with the same thickness and the same nose coefficient are connected by curves. The various profile thicknesses are marked by various plottings of the points and the nose coefficients by different plottings of the lines. The increase of  $C_D$  with the profile thickness in the case of constant nose coefficient and backward position of thickness is due to the thickening of the turbulent boundary layer in the rear

part of the profile; for the transition point will not move considerably in this case. For the profiles with the three smaller nose coefficients we observe a considerable decrease of  $C_D$  with increasing backward position of thickness. This is due to the prolongation of the laminar boundary layer. This is no longer the case, however, for the usual nose coefficient 1.1 of NACA-profiles. In at least 2 of the four indicated cases the most favourable backward position of the thickness is below 50 per cent. of the chord. Hence it is indispensable if we want to develop a profile with a pronounced laminar effect from a standard profile, to decrease the nose radius as well as to displace the maximum thickness backwards. Since this is necessarily connected with a loss of maximum lift, we shall naturally try to manage with a minimum reduction of the nose radius.

#### 4.124 The Laminar Effect and the Range of Lift. Influence of the Profile Camber.

The pressure distribution being of decisive influence on the position of the transition point, great backward positions of the latter can exist in a  $C_L$ -range only in which no considerable sub-pressure peaks were found near the nose. According to the available measurements this was generally the case in a range  $C_L = 0.2$  to  $0.3$  for not too small nose radii. Fig.4 shows a striking example for the position of the transition point and the drag coefficient. It refers to the laminar profile indicated in Fig.2 [4].

For the same reason we can suppose that the  $C_L$ -range of great backward positions of the transition point moves towards higher  $C_L$ -values with increasing camber. As is shown by the measurements, [4], this  $C_L$  range always lies on both sides of the entry without shock waves, i.e. of the  $C_L$ -value for which the stagnation point lies at the point of intersection of the skeleton line with the contour of the profile. Moreover the transition point on the suction side moves forwards more gradually in the case of cambered profiles than in the case of the symmetrical profile, \* of the influence of the camber on the position of the transition point enabled us to restrict the investigations on laminar profiles to symmetrical profiles which is obviously an essential simplification.

\* whereas the motion of the pressure side remains sudden [4].  
This knowledge



#### 4.13 Influence of the Position of the Transition Point on the Lift.

We have so far discussed only the influence of the position of the transition point on the resistance. The desired great backward positions of the transition point could only be maintained in a relatively small  $C_L$ -range. At the limits of this range the transition point began to move forwards more or less quickly on one of the profile sides. This forward movement has an unfavourable influence on the lift. In order to explain this let us again first consider the flat plate.

##### 4.131 The "Lift Jump" on the Flat Plate.

We assume symmetrical flow and the boundary layer on both sides of the plate to be laminar up to the trailing edge. Let us laminar thickness of displacement on both sides of the trailing edge be  $\delta_{1l}$  (compare Fig.5, case (b)). With a very small angle of incidence in the one or the other direction which will not considerably vary the pressure distribution of the potential flow, the transition point jumps on the respective suction side to the leading edge of the plate.

At the trailing edge of the respective suction side there will then be the - mostly much greater - thickness of displacement of the turbulent boundary layer  $\delta_{1t}$  (case (a) and (c) of Fig.5). The mean point of departure of the streamlines for different thicknesses of displacement  $\delta_{1l}$  and  $\delta_{1t}$  is  $0.5 (\delta_{1t} - \delta_{1l})$  above or below the trailing edge of the plate. Thus a small angle of incidence  $\alpha_{ind.} \approx 0.5 (\delta_{1t}/c - \delta_{1l}/c)$  is induced. If the plate now passes at  $\alpha = 0$  the conditions (a), (b), (c) of Fig.5 one after another starting with negative and ending with positive angles on incidence, the effective angle of incidence makes a jump amounting to  $2\alpha_{ind.}$ . From this results a jump of the lift coefficient  $C_L$  amounting to  $\Delta C_L = 4\pi\alpha_{ind.}$ , and the lift coefficient plotted against the geometrical angle of incidence is represented by Fig.5 (d). Using the well-known Blasius formula for the laminar and the turbulent thickness of displacement at the trailing edge, we obtain the relation

$$\Delta C_L = 0.29 \cdot R^{-0.2} - 10.9 \cdot R^{-0.5}$$

for the "lift jump" as we shall briefly call it.

8

Fig.6 shows the lift jump plotted against the Reynolds number of the plate according to this formula. As is seen, the lift jump at the flat plate is not very great. The maximum value is about 0.008 and corresponds to about  $R = 3 \times 10^6$ . With increasing R-number  $\Delta C_L$  decreases only slowly and hence the R-numbers, nowadays usual for aeroplanes, remain in the range of the maximum. Below the R-numbers of the maximum the value of the lift jump quickly drops to zero. Negative values of  $\Delta C_L$  are unimportant, since according to experience the boundary layer on the plate is not yet turbulent for the associated small R-numbers.

#### 4.132 The "Lift Jump" for Profiles.

As is seen above, the lift jump necessarily is involved by the movements of the transition points if these movements do not run at the same time and in the same sense. Since the movements of the transition points, however, do not run in the same sense when changing the angle of incidence, all laminar profiles have a lift jump, too. This lift jump is often considerably greater for profiles of finite thickness than for the flat plate. This is due to the fact that the turbulent boundary layer extends during pressure rise by a far greater part up to the trailing edge than the laminar one and thus contrary to the flat plate the mean point of departure of the streamlines is additionally displaced towards the suction side due to the pressure rise.

Fig.7 shows the lift jumps of some symmetrical laminar profiles. The symmetrical profiles of the enlarged NACA systematics already known from Fig.3 were again chosen as examples [5]. The values of the ordinates were gained from the measured  $C_L(\alpha)$ -curves by linear extrapolation from the straight part of the curve towards  $\alpha = 0$ . As is seen lift jumps of 40 fold the maximum value calculated for the flat plate were measured in extreme cases. Since, according to the above mentioned facts they are chiefly caused by the thickness of the turbulent boundary layer at the trailing edge, we had to suppose from the very beginning that the profiles with greatest pressure rise, i.e. with great thicknesses, show the greatest lift jumps. The figure confirms this behaviour. With decreasing thickness of course, the influence of the backward position of thickness must decrease, too, until it vanishes completely at the thickness 0. This behaviour is shown in Fig.7: the slope of the curves decreases with decreasing thickness.

#### 4.133 The Shapes of the Lift Curves.

Not only the lift jump is important, i.e. the difference of ordinates between the two straight branches of the  $C_L(\alpha)$ -curve running parallel to each other, but the shape of the transition curve between the two branches is important, too. The discontinuous transition from the lower to the upper branch shown in Fig.5, (d), can always be realized artificially, say, by means of suitable disturbing wires. Without such a trick, however, the transition is continuous within a more or less great range of  $C_L$ .

Fig.8 shows the four possible typical shapes of the  $C_L$ -curves plotted against the angle of incidence in the case of symmetrical laminar profiles.

Case (a) is the usual case for profiles with good laminar properties; within a range about  $C_L = 0$  the transition points mainly lie in the rear part of the profile and do not move (as in Fig.4). Above a certain  $C_L$ -value the transition point on the suction side begins to move forwards. As we can conclude from the above considerations, this movement will continuously cause infinitesimal lift jumps, i.e. a decrease of  $dC_L/d\alpha$ . Only when the transition point on the suction side has reached its final position with farther increase of the angle of incidence,  $dC_L/d\alpha$  will again increase to its usual value. In cases with great angle of the trailing edge (i.e. great thickness and great backward position of thickness) the boundary layer at the trailing edge already becomes so thick during the forward movement of the transition point that the increase of lift is overcompensated by the increase of the angle of incidence, and  $dC_L/d\alpha$  becomes negative. This considerably more unfavourable case is represented by curve (b) of Fig.8. It is near at hand and was successfully tried to avoid this case by sucking off the boundary layer at the rear part of the profile [2]. Case (b) could be transferred to case (a) already with a relatively small sucked quantity. Thus not only negative  $dC_L/d\alpha$  is obviously avoided, but the lift jump  $\Delta C_L$  is decreased, too.

Contrary to (a) and (b) the cases (c) and (d) of Fig.8 occur, when the counter-movements of the transition points already begin with zero angle of incidence. This is the case for the laminar profiles with relatively thick noses, for instance with all profiles of Fig.7 which have the nose coefficient 1.1, whereas the profiles with the nose coefficient 0.825 already belong to type (a)

or (b), respectively (d) occurs instead of (c) in the same cases as (b) instead of (a). Only the two thickest profiles of Fig.7 with a backward position of thickness of 50 per cent. are associated to type (d).

They would probably be improved by suction, too. Improvements could also be shown by artificial reduction of the angle of the trailing edge by means of hollow profile flanks at the rear part [8, 26].

#### 4.14 Influence of the Position of the Transition Point on the Aerodynamic Centre and the Neutral Point.

The above discussed irregularities of the lift curves must at the same time produce irregularities in the curves of moments. Here, however, the influence of the displacement of the transition point on the position of the aerodynamic centre has still to be considered. If e.g. the transition point advances on the upper side of the profile with positive angle of incidence losses of sub-pressure will result in the rear part of the profile by the relatively great thickness of displacement. The point of attack of the resultant lift force is thus displaced forwards, in other words: symmetrical profiles with no fixed transition points have no fixed aerodynamic centres either. In spite of this the pressure points of symmetrical standard profiles with their slight movements of the transition points can be practically considered as constant. This is not the case, however, for laminar profiles. Let us choose as extreme case. The movement of profiles with the lift curve of the type of Fig.8 (d), for instance, is only zero for central passing of the zero point, while a finite negative or positive diving moment, respectively, exists for left or right passing of the zero point. For reasons of symmetry both diving moments have the same amount. They can assume considerable values: The two profiles in Fig.7 with lift curves of the type 8 (d) (nose coefficient 1.1 and backward displacement of thickness of 50 per cent.) have coefficients of diving moment of 0.07 for 18 per cent. thickness and 0.04 for 15 per cent. thickness [5].

On account of this influence of the position of the transition point on the curve of moments it suggests itself to develop profiles for which theoretically, i.e. when neglecting the friction layer, the movement of the aerodynamic centre is just opposite to the influence of the displacement of the transition point, so that

a balancing effect can be obtained in the average within a given  $C_L$ -range. For such investigations we have to take into consideration, of course, that, for practical flight conditions the R-number of the aerofoil depends on the  $C_L$ -value. Developments in this direction have not become known so far. The displacement of the transition point influences also the position of the neutral point. The neutral point is that point of an aerofoil profile which, chosen as point of reference of moments, causes the smallest possible change of the moment coefficient with the lift coefficient. The Mustang-profile seems to have passed a development with the aim of constant position of the neutral point [8]. According to measuring results this favourable property of the Mustang-profile no longer prevails when the hollow flanks in the rear part of the profile are filled up until a straight shape is obtained. At the same time this increase of the angle of the trailing edge involves an increase of the lift jump  $\Delta C_L$  [26].

#### 4.15 Influence of the Reynolds Number on the Position of the Transition Point.

The test results with laminar profiles considered so far were gained from wind-tunnel tests with R-numbers from 2 to  $3 \times 10^6$ . The decisive question is now how these laminar profiles behave for R-numbers of practical flight which are higher by about a power of tenth order.

The well-known theory of small disturbances (compare B 3) yields the stability limit for a profile with laminar boundary layers to be a certain R-number which depends on the shape of this profile. Below this critical R-number small disturbances are always damped, above it, disturbances within certain ranges of frequency might be excited. The actual transition point, however, will often still occur at a R-number which is many times the R-number characterized by the limit of stability. On the other hand no cases are known so far where the transition point measured is below the limit of stability so that the latter can be considered to be the lowest limit of the R-number for the position of the transition point. It would be desirable to obtain a relation between the actual positions of the transition points and the parameters of excitation given by theory by means of systematic extensive measurements of profiles with critical boundary layers made in a flow with lowest possible turbulence and by comparing the results with theory. Thus it would be

possible to predict the positions of the transition points for any profile at any angle of incidence and for any R-number, without measurements.

Measurements with R-numbers of the order of  $20 \times 10^6$  were made on two profiles only.

One is a symmetrical J o u k o w s k i - profile of 15 per cent. thickness and a backward position of thickness of 60 per cent. [23]. It showed a very favourable pressure distribution. The measurement in the great wind-tunnel of Völkenrode yielded an increase of the drag coefficient beginning at about  $R = 5 \times 10^6$ , and the  $C_D$ -value of standard profiles was already reached at  $R = 10 \times 10^6$ . In the same way as this  $C_D$ -value was adapted to that of standard profiles, the lift curve was smoothed, i.e. the lift jump was reduced. Both means involve an advance of the transition point in the forward part of the profile.

The other profile measured for similar R-numbers is the so-called "Russian laminar profile" [25] (12 per cent. thickness, 50 per cent. backward position of thickness and camber, 1 per cent. camber, nose coefficient 0.21). From the pressure distribution and the calculation of stability [17] can be seen that it is inferior to the above-mentioned J o u k o w s k i - profile with respect to the laminar properties, nevertheless it was measured, since a Russian measurement was said to have stated good laminar properties even at  $R = 18 \times 10^6$  ( $C_D = 0.003$ ). This Russian test result, however, could neither be confirmed in the wind-tunnel at Göttingen nor at Völkenrode. Increases of the  $C_D$ -values of similar order of magnitude and within the similar range of R-numbers as for the Joukowski-profile resulted from these measurements.

The influence of the degree of turbulence which is about the same for the wind-tunnel of Göttingen and Völkenrode remains still unknown in the case of these measurements. [14]. This influence can only be specified by measuring the same laminar profiles in the tunnels and for comparison in free flight or in a non-turbulent airstream. Such measurements were not made so far in Germany. We can not answer the decisive question if suitable laminar profiles can be realized for R-numbers of modern aeroplanes.

#### 4.16 Maintenance of the Laminar Conditions by means of the Shape of the Aerofoil.

We have so far discussed the maintenance of laminar conditions by means of a suitable choice of the aerofoil profile. In principle, however, it is also possible to obtain laminar effects by using special shapes of the aerofoil itself whereas the usual profile is kept.

An example is given by the corrugated sheet aerofoil as is shown in Fig.9. The profile of the aerofoil is the same in each section. The angle of incidence of the profile, however, changes in spanwise direction according to a sine curve, where the single profiles are turned about the nose as axis. The design of this aerofoil was based on the idea that material of the boundary layer will flow from the crests into the troughs on both sides. This downward flow has a similar effect as a suction (compare 4.2) has on the residual boundary layer on the crests, i.e. it will probably cause a longer maintenance of the laminar conditions. On the other hand the turbulent boundary layer in the troughs is thickened by the downward flow. On the crests as well as in the troughs, therefore, we can expect the reduction of the resistance of the boundary layer. Though the test results [27] confirmed these reflections in principle, no resistance was saved as compared with the non-corrugated sheet-aerofoil of comparison since the frictional surface is increased owing to the corrugated sheet, on the other hand the drag curve along the span reached its maximum values just at those points, to which the above reflections do not refer, namely at the zero points of the sinusoidal trailing edge-curve.

A laminar effect could also be stated qualitatively for swept-back aerofoils as compared with non-swept-back aerofoils of the same profile [6, 24]. According to the test results this effect is probably not due to the moment of the material of the boundary layer from the root towards the tip, but it will be caused by the decrease of the super-velocities due to the sweep-back.

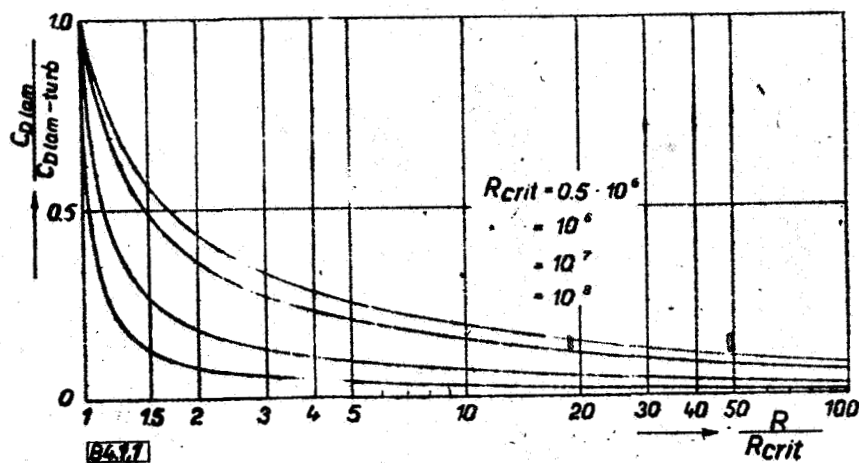


**Fig.1:** Diagram for the calculation of the savings of resistance by the backward displacement of the transition point up to the trailing edge for a flat plate in parallel flow.

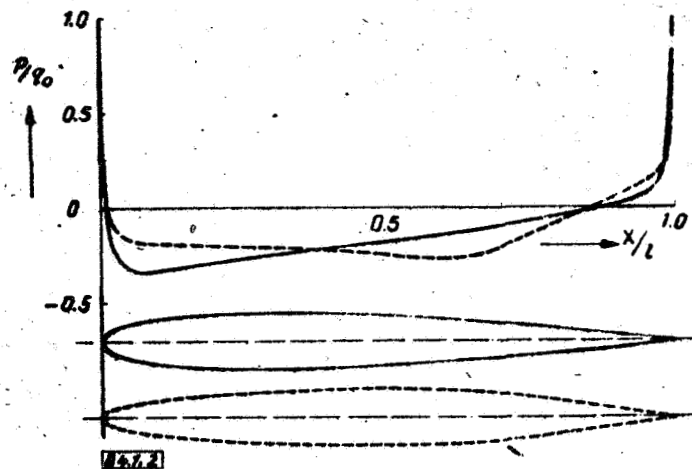


**Fig.2:** Comparison of the pressure distribution of the profile NACA 0010 (backward position of thickness 30 per cent.) with that of a laminar profile of the same thickness and a backward position of thickness of 50 per cent.



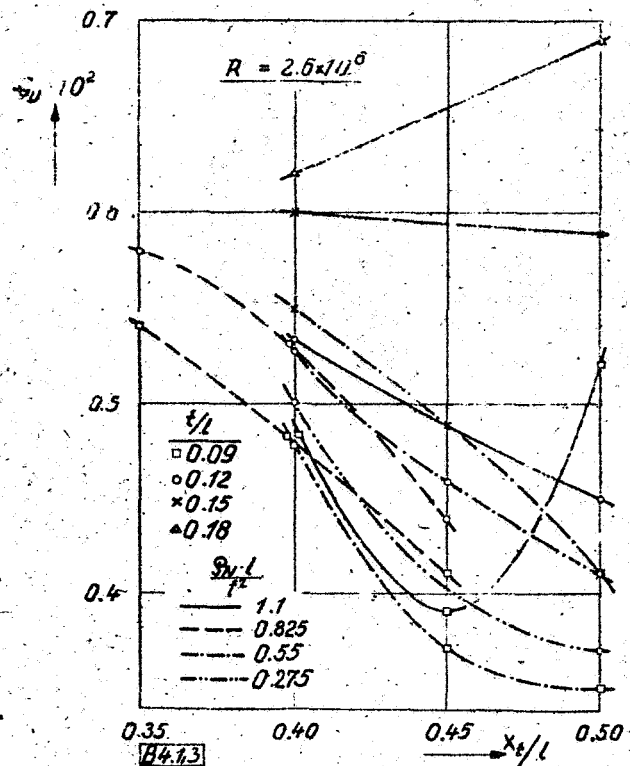


**Fig.3:** Drag coefficient of symmetrical laminar profiles of an enlarged NACA systematics in function of thickness, backward position of thickness, and nose coefficient.

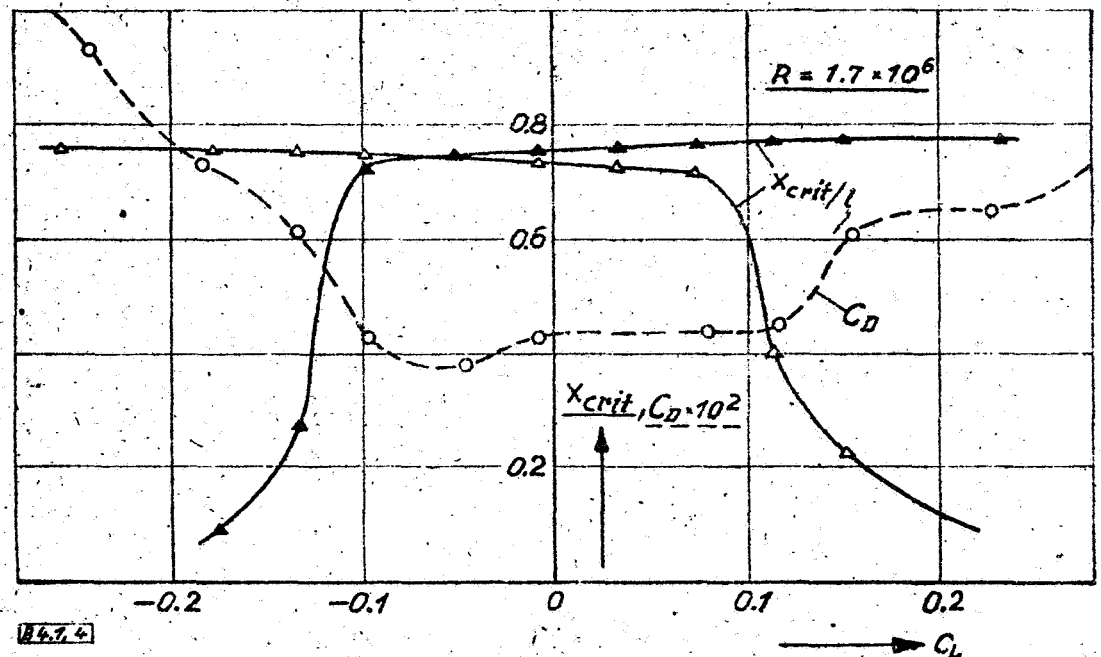


**Fig.4:** Typical behaviour of the position of the transition point on the upper and the lower side and drag coefficient for a symmetrical laminar profile (profile shape compare Fig.2) in the range of small lift coefficient.

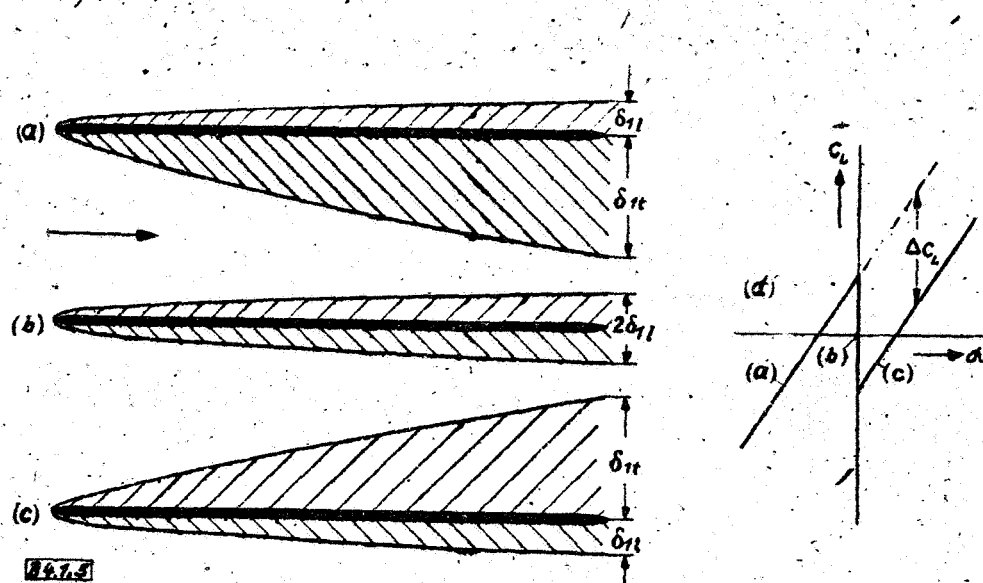


Fig. 5: To the deduction of the "lift-jump" on the flat plate, ordinates in a, b, c are drawn in a considerably enlarged scale.

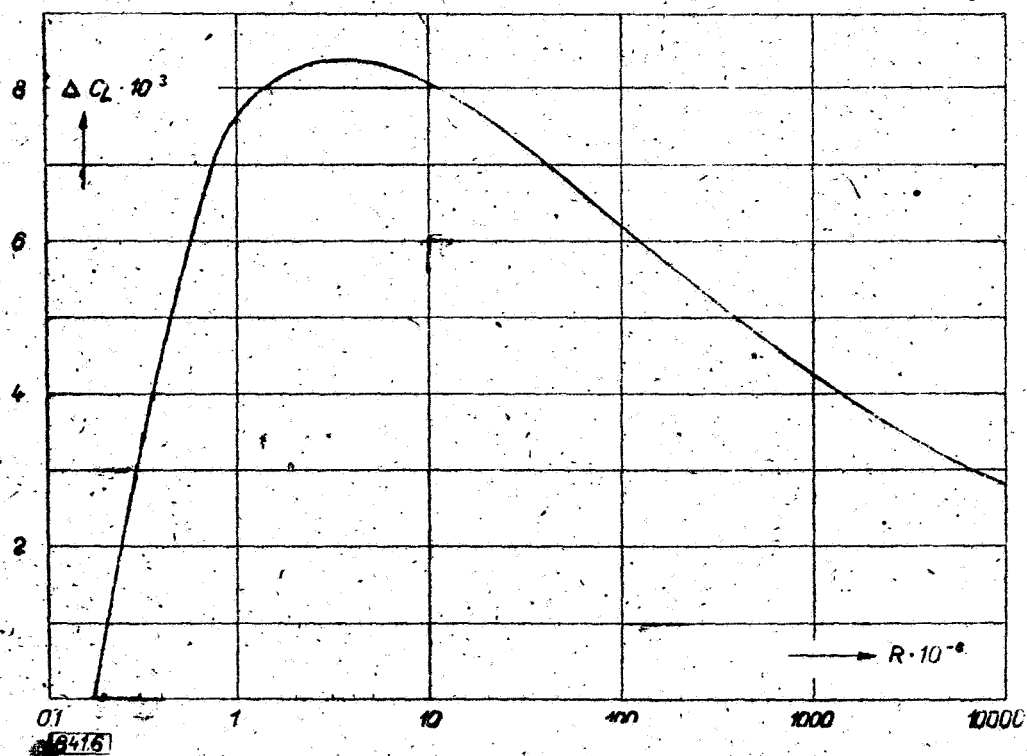
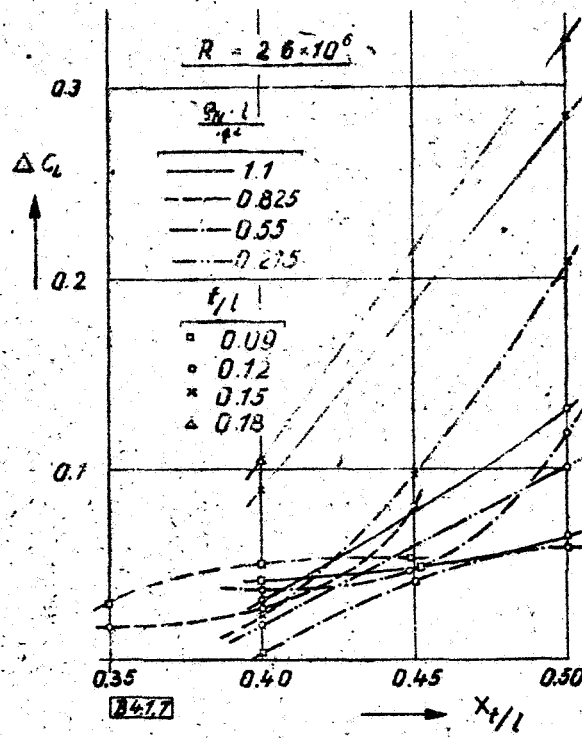
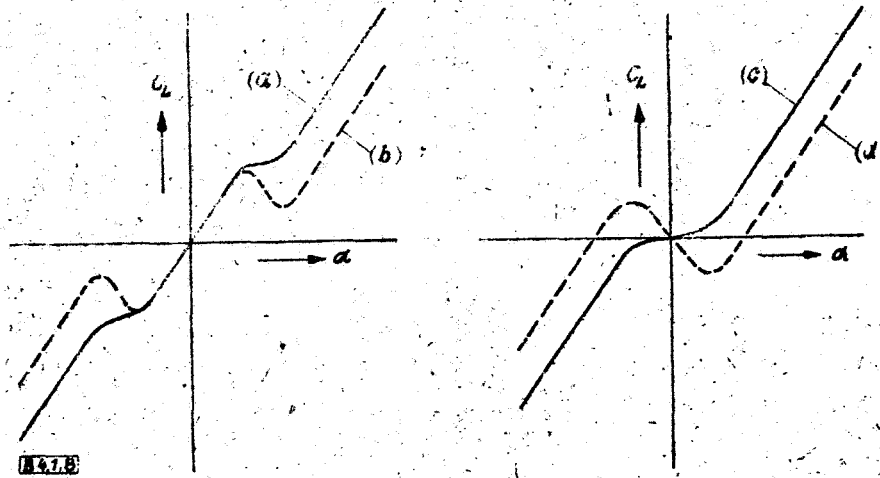


Fig. 6: The lift jump against the Reynolds number for the flat plate.



**Fig.7:** The lift jump for the laminar profiles of Fig.3 in function of thickness, backward position of thickness, and nose coefficient.



**Fig.8:** Possible shapes of the lift curves against the angle of incidence.

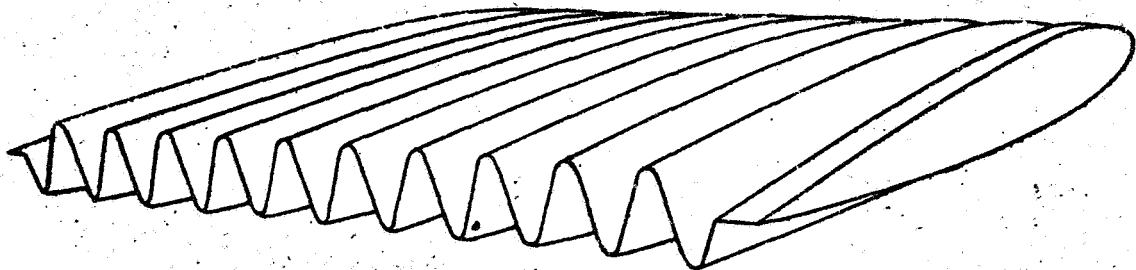


**Fig.9:** Sketch of a corrugated sheet aerofoil.

## 4.2 Maintenance of the Laminar Conditions by Suction.

By H.Holstein.

### 4.21 Survey and Limitation.

As was shown in the preceding section, the problem to obtain laminar conditions by a suitable choice of the body shape leads to considerable alterations as against the usual shapes.

Due to these changes other aerodynamic properties were necessarily deteriorated at least when these bodies, as for instance the aerofoil profile, had reached a high state of development. It is therefore important to have other means, too, which enable us to maintain the laminar conditions without requiring changes of the shape. Such a means is given by the suction of parts of the boundary layer.

There is a double effect of the suction on the boundary layer. First: the boundary layer is reduced in size by taking away flow material. Thus every Reynolds number formed by means of a boundary layer parameter, for instance the thickness of displacement, is artificially reduced, too. Secondly: the shape of the boundary layer is also altered, for, due to suction those layers are removed which are nearest the wall i.e. which are most considerably braked, and the profile of the boundary layer becomes more convex. Both alterations, the reduction of Reynolds number as well as the change of the shape at the boundary layer profile have a stabilising influence according to the results of the stability theory for laminar boundary layers (compare B 3). Thus the suction seems to be promising to keep laminar conditions.

The suction can be so great that it influences the pressure given by the potential flow by producing a particular field of sinks. This would be an additional favourable effect for the stabilization of the boundary layer as is easily seen. For the present purpose, however, such intense suction do not prove favourable, therefore, they will not be discussed here.

### 4.22 Formulations of Notions and Evaluation Formulae.

When using suction the problem of possible gains in propulsive power is not so easy to survey as when using suitable shapes of the body in order to keep laminar conditions; for, suction generally consumes power and this must be taken into con-

sideration when drawing the final power balance. Moreover the sucked air must be blown out again and this will generally require additional acceleration power. In the case of suction, therefore, the drag coefficient  $C_D$  is replaced by the so-called coefficient of profile efficiency  $C_{perf.}$  as characteristic quantity for the calculation of the propulsive power. For a long time it has usually been indicated in the form [28]

$$C_{perf.} = C_D + \sum_n C_{qn} (1 - C_{pn}) . \quad (1)$$

Where  $n$  is the number of suction slots and  $C_{qn}$  is the coefficient of the quantity sucked through the slot  $n$  made non-dimensional by the velocity of the incident flow and a suitable surface of the body (for aerofoils the supporting surface)  $C_{pn}$  denotes the overpressure in the suction chamber associated to slot  $n$  as against the undisturbed static pressure. It is referred to the undisturbed dynamic pressure. Formula (1) is based on the following suppositions:

- 1) Hydraulic losses in the suction and blowing off pipes can be neglected.
- 2) Propulsion-, suction- and blowing off unit have the same efficiency.
- 3) The air is blown out at flying speed and at a point of undisturbed static pressure.

Moreover the definition of the drag coefficient  $C_D$  in the above formula is important: it is the value resulting from the depression of the momentum curve behind the aerofoil without blowing out. It vanishes for instance, when the whole turbulent boundary layer is sucked at the trailing edge whereas the drag coefficient resulting from the integral of the shearing stress and the pressure distribution would naturally not vanish. The difference between the two is called "sink resistance".

In all cases in which we try to save propulsive power it is therefore not sufficient according to the above facts to keep the boundary layer laminar by means of suction. Besides the associate power percentages must remain so small that we obtain a considerable advantage as compared with the aerofoil without suction when these values are taken into consideration according to formula (1).

The pressure coefficient obviously depends on the outside pressure at the suction slot as well as on the geometry of all

-20-

parts between the outer contour and the suction chamber which are passed by the sucked material. It could be proved in a series of tests with different arrangements and widths of the slots [32] that it is always possible within the range of the relatively small suction quantities used for the purpose in question to keep the pressure in the suction chamber equal to the outside pressure by suitable construction. These tests were made on a flat plate and, strictly speaking are only valid for the boundary layer profile of the flat plate according to B l a s i u s . No remarkable alterations of these test results, however, will be expected for laminar boundary layer profiles in the pressure drop or pressure rise, if these profiles do not differ too much from Blasius' profile. The pressure coefficient  $C_p$ , therefore, can be taken with sufficient approximation from the outside pressure in the case of aerofoils if the parts passed by the flows are well designed as to their hydraulic properties.

We can thus make relatively reliable predictions on the amount of the pressure coefficient required, this is, however, much more difficult concerning the volume coefficient.

In practice a certain part of the profile chord will generally be given along which the laminar conditions shall be kept by suction.

This part can be provided either with many or few slots. In the latter case relatively greater volumes must of course be sucked by each slot. The question will then be: in what case is the coefficient of the total suction volume smaller

$$C_Q = \sum_n C_{Qn} \quad (2)$$

The few tests so far available on the laminar conditions kept by suction seem to indicate that the main difficulty is not to keep the flow laminar but to keep the required suction volumes small enough.

In order to clear these problems let us again discuss the flat plate which at the same time will enable us to consider the test results to be dealt with later on critically and to avoid mistakes when judging future tests. Let us already mention here that the pressure coefficient for the flat plate can always be put equal to zero according to the above test results. Considering (2) the formula (1) for the flat plate is thus simplified to

$$C_{\text{perf.}} = C_D + C_Q \quad (3)$$

#### 4.23 Theoretical Reflections on the Flat Plate.

##### 4.231 An Approximation Formula for Suction at the Flat Plate.

Let us consider a flat plate in parallel flow according to Fig.1. The velocity of the incident flow be  $U_0$ , and the chord of the plate  $l$ . Let the laminar boundary layer reach its critical thickness of displacement  $\delta_{1crit.}$  at the point  $X_{crit.}$  where the transition takes place. Here a suction slot will be arranged through which a volume  $Q_n$  is sucked from the boundary layer and thus the transition will be prevented at this point. After suction - which makes the thickness of displacement decrease, the latter will increase again until it reaches the value  $\delta_{1crit.}$  again at a distance  $d$  behind the first suction slot. Here a new suction slot will be arranged, and the volume  $Q_n$  will be sucked again. This method will be continued as far as the trailing edge of the plate. Let thus arise  $n$  slots. Then the chord  $l$  can be written as:

$$l = X_{crit.} + n \cdot d \quad (4)$$

whereas

$$C_Q \cdot U_0 \cdot l = Q = n \cdot Q_n \quad (5)$$

holds for the coefficient of the sucked volume  $C_Q$  according to the definitions.

In order to consider the conditions of the suction slot itself we choose the simplest arrangement from the theoretical point of view as given in Fig.2. The slot is overlapped and the rear slot lap is infinitely thin and parallel to the flat plate. By suitable balancing the height of overlapping  $Y_s$  and the suction volume  $Q_n$  that the incident becomes symmetrical in flow. Let the velocity at the height  $Y_s$  be  $u_s$ .

For simplification of the calculation we assume after Blasius the laminar velocity profile of the flat plate (dashed line in Fig.2) to be replaced by a "triangular profile" of equal skin friction stress. (Fig.2).

For such a profile we then obviously have:

$$\left( \frac{\partial u}{\partial y} \right)_{y=0} = \frac{u_s}{Y_s} = \frac{U_0}{2\delta_1} \quad (6)$$

Whereas the velocity gradient at the wall is given due to Blasius by

$$\left(\frac{\partial u}{\partial y}\right)_{y=0} = k \cdot U_0 \cdot \sqrt{\frac{U_0}{\nu \cdot x}} \quad (k=0.332) \quad (7)$$

which also holds in the present case according to the presupposition. From (6) and (7) result the thickness of displacement  $\delta_1$  and the height of overlapping  $Y_s$ :

$$\delta_1 = \frac{1}{2 \cdot k} \sqrt{\frac{\nu \cdot x}{U_0}} \quad (8)$$

$$Y_s = \frac{1}{2 \cdot k} \sqrt{\frac{\nu \cdot x_{krit.}}{u_s}} \quad (9)$$

Two further relations can be taken from Fig.2: The sucked volume  $Q_n$  is

$$Q_n = \frac{u_s \cdot Y_s}{2} \quad (10)$$

and the reduction  $\Delta \delta_1$  of the thickness of displacement due to suction can be taken from

$$U_0 \cdot \Delta \delta_1 = U_0 \cdot Y_s - Q_n \quad (11)$$

Now we need a supposition on the re-increase of the thickness of displacement, reduced by suction, behind the slot. Obviously the velocity  $U_0$  at the border of the boundary layer as well as the velocity  $u_s$  at the overlapping height (compare Fig.2) influence the value of this increase. These facts suggest the following approximate supposition: The thickness of displacement increases after suction as on the leading edge of a flat plate with a mean velocity of its incident flow of  $0.5 (U_0 + u_s)$ . With this supposition we have, analogous to (8), for the increase  $\Delta \delta_1(x)$  after the suction as far as a point X between the first and the second suction slot

$$\Delta \delta_1(x) = \frac{1}{2 \cdot k} \sqrt{\frac{\nu \cdot (x - x_{crit.})}{0.5 (U_0 + u_s)}} \quad (12)$$

According to the presuppositions (compare Fig.1) made on the suction, the thickness of displacement at the second slot, i.e.,



at  $x = x_{crit.} + d$ , will be equal to that directly in front of the first slot. This means, however, that the increase  $\Delta \delta_1(x)$  at this point must be equal to the decrease  $\Delta \delta_1$  given by (11). Hence the expression

$$\Delta \delta_1 = \frac{1}{2k} \sqrt{\frac{\nu \cdot d}{0.5(U_0 + u_s)}} \quad (13)$$

resulting from (12) for the special case  $x - x_{crit.} = d$  can be inserted in (11) for  $\Delta \delta_1$ . Then  $Y_s$  and  $u_s$  can be eliminated by means of (9) and (10), and according to (5) the coefficient of the sucked volume  $C_Q$  can be introduced instead of  $Q_n$ . If the number of slots  $n$  is eliminated, too, in this new equation by means of (4) and if we introduce the abbreviations

$$\frac{U_0 \cdot l}{\nu} = R_i \quad \frac{U_0 \cdot x_{crit.}}{\nu} = R_{crit.}; \quad \frac{U_0 d}{\nu} = R_d \quad (14)$$

$$\frac{\sqrt{R_{crit.}} C_Q}{1 - R_{crit.}/R} = f(z); \quad \frac{R_d}{R_{crit.}} = z \quad (15)$$

we finally obtain

$$2k^2 f(z) \left( \sqrt{\frac{2}{k}} - \sqrt{z f(z)} \right)^2 \cdot (1 + \sqrt{2k z f(z)}) - 1 = 0 \quad (16)$$

It represents the required dependence of the coefficients of the sucked volumes  $C_Q$  on the  $R$ -numbers defined by (14).

#### 4.232 Discussion of the Approximation Formula (16).

The value  $z$  occurring in (16) obviously is the ratio of the slot distance to the running length of the laminar flow. Therefore  $z$  can vary within the range  $0 \leq z \leq 1$  only. The limiting case  $z = 1$  exists when the distance of the slots has its maximum value. In this case the whole boundary layer is sucked and we obtain from (16)

$$f_{(z=1)} = \frac{1}{2k} = 1.506 \quad (17)$$

The other limiting case ( $z = 0$ ) is under discussion when the slots are arranged at infinitely small distances. In this case of the so-called continuous suction we obtain from (16)

$$f_{(z=0)} = \frac{1}{4k} = 0.753 \quad (18)$$

i.e. just half the value of the limiting case (17). The curve of  $f(z)$  between these two limiting values is represented in Fig.3. It shows a curve with increasing slope.

Since approximative suppositions the admissibility of which is not quite clear were made for the deduction of  $f(z)$ , it seems first to be necessary to discuss the curve given by  $f(z)$ .

The limiting case (18) of the continuous suction of the boundary layer on the flat plate can also be exactly calculated from Prandtl's equation of the boundary layer. (Compare [30]). The exact solution gives the numerical value 0.664, instead of (18) hence satisfactory agreement. On the other hand the increasing slope from its value at  $z = 0$  given by (18) can also be understood immediately. According to suppositions the boundary layers directly behind the slot are always smaller in the case of great slot distances. Small boundary layers, however, grow more quickly along a certain distance than great boundary layers. If a given slot distance is increased, the increase of the boundary layer thickness and with it of the suction volume required is the greater, the greater the given distance of the slots. Thus the initial point and the increasing slope of the curve given by Fig.3 are ensured. As to the value at the other point  $z = 1$  given by (17), the approximative supposition (12) on the increase of the thickness of displacement behind the slot obviously becomes quite correct for the "triangular" boundary layer; for the whole boundary layer is sucked in this case and thus  $u_s = U_0$ . Hence the boundary layer begins behind the slot just as at the leading edge of a flat plate with a velocity  $U_0$  of the incident flow. Here an error is involved only by the fact that the Blasius boundary layer profile was replaced on the flat plate by a triangular profile of equal skin friction stress. As is easily seen with Blasius' profile by graphical integration, the suction given by (17) covering the whole boundary layer profile corresponds to a suction on Blasius' profile as far as a velocity of about  $u_s = 0.85 U_0$ . Hence a small thickness of displacement would be left in this case behind the suction slot. If we wanted, however, to suck the boundary layer completely, an infinitely great suction volume would be required according to Blasius owing to the mere asymptotical tran-

-25-

sition into the frictionless flow. As against the suction as far as  $U_s = 0.85 U_0$  the slot distance, however, would thus increase by 1 per cent. only, as can easily be confirmed by calculation. Hence the curve of Fig. 3 gained by means of Blasius' profile would have a vertical tangent at  $z = 1$  and the value given by (17) would be already reached at about  $z = 0.99$ . The difference between both curves is practically unimportant. Hence the approximation formula (16) seems to be sufficiently reliable.

Let us now investigate the important problem concerning the dependence of the coefficient of the suction volume on the R-number with the help of the formula. This can be done by means of Fig. 4 where  $\sqrt{R_{crit.}} \cdot C_Q$  is plotted against  $R/R_{crit.}$  for different parameters  $R_d/R_{crit.}$  or  $R_d/R$ , respectively. If  $R_{crit.}$ , i.e. that R-number for which the transition would take place without suction, is considered as constant, this diagram directly indicates the dependence of the volume coefficient on the R-number.

Along the full lines  $R_d/R_{crit.} = z$  is the constant parameter, the final values 0 and 1 as well as the value 0.75 being chosen corresponding to a line lying about the middle of the two other. The rise of the curves with increasing abscissa from  $C_Q = 0$  is caused by the fact that a continuously greater portion of the plate is provided with suction. The limiting values for infinitely great abscissa are marked by circles. When assuming the R-number only to be increased by the increase of the chord  $l$ , these curves are valid for a fixed slot distance  $d$ . Hence they give the progress of the volume coefficient when the rear part of the plate is continuously enlarged piece by piece. If the chord, however, is kept constant and the velocity of the incident flow  $U_0$  increases, the slot distance  $d$ , at fixed  $R_{crit.}$ , had to be varied proportional to  $1/U_0$ , if the curves shall remain valid.

The dashed curves of Fig. 4 hold for fixed values of the parameter  $R_d/R$ . The product of parameter and abscissa is  $R_d/R_{crit.} = z$ , hence at most equal to unity. These curves must therefore end at abscissae which are equal to the reciprocal value of their parameters. Moreover they end on the upper of the full curves above discussed which holds for  $z = 1$ . When assuming the abscissa to be increased by the increase of the chord  $l$ , the slot distance will also increase proportional to  $l$  along these dashed curves, hence they give the variation of the volume coefficient with similar enlargement of the model. If, on the other hand, we increase the

abscissa by increasing the velocity of the incident flow and we keep the chord  $l$  constant, the slot distance  $d$  will also remain constant with these curves. Hence they also give the variation of the coefficient of the suction volume necessary for keeping the laminar conditions for a given model whose velocity of incident flow is increased.

As is seen from these statements, the dependence of the volume coefficient on the  $R$ -number is manifold and we can survey it only after introducing further conditions. The coefficient of suction volume will generally increase with the  $R$ -number if quick decrease of the slot distance with increasing  $R$ -number is not assumed as particular condition. This is a disadvantage growing with great  $R$ -numbers, since as is known the drag coefficient without suction decreases with increasing  $R$ -number.

The number of slots  $n$  can be calculated in any case from Eq.(4) which can be easily changed into the form

$$n = \frac{R/R_{crit.} - 1}{Rd/R_{crit.}}$$

or

(19)

$$n = \frac{1}{Rd/R} \left( 1 - \frac{1}{R/R_{crit.}} \right)$$

The former equation can be suitably used for the full curves and the latter for the dashed curves of Fig.4. For a better survey curves of constant numbers of slots  $n$  were not drawn in Fig.4.

After the volume coefficient is given by formula (16) or Fig.3, respectively, the power coefficient  $C_{perf.}$  can also be calculated by means of Eq.(3).

As in section 4.1  $C_{D \text{ lam.-turb.}}$  be the drag coefficient of a flat plate without suction with a transition point corresponding to  $R_{crit.}$ . As against such a plate the relative saving of propulsive power which results from keeping the laminar conditions from the above transition point up to the trailing edge by means of suction is then obviously

$$1 - \frac{C_{perf.}}{C_{D \text{ lam.-turb.}}}$$

It can be easily taken from Figs.5 and 6 for R-numbers between  $10^6$  and  $100 \times 10^6$ . With respect to the parameters Fig.5 corresponds to the dashed curves and Fig.6 to the full curves of Fig.4. As is seen all the curves have minima which correspond to the greatest possible savings of propulsive power. At R-numbers above these minima the increase of the coefficient of suction volume together with the decrease of the drag coefficient without suction causes again a decrease of the power savings. For sufficiently great R-numbers, therefore, the curves of Fig.5 increase beyond unity. This, however, is only the case for very high R-numbers which are not yet of interest in practice nowadays. The ends of the curves of Fig.6 again correspond to the suction as far as the 85 per cent. limit of the velocity of Blasius' boundary layer profile. According to the above considerations we have normal tangents and hence poles of the curves. For a design it is of course important already to take into consideration that suction will never occur in the range of such poles even at the highest R-number in question.

#### 4.24 The Tests Carried out so far.

Three different wind-tunnel tests were made in Germany concerning the problem of keeping the boundary layer laminar by means of suction.

The first [29] was made on a symmetrical v.Kármán-Trefftz-profile of 15 per cent. thickness and a backward position of thickness of 33 per cent. On both sides 10 suction slots each with rounded slot edges were arranged over the whole span at equal distances. The R-number for this test was  $1.6 \times 10^6$ . Material of the boundary layer was sucked with the most various combinations of these slots, and at the same time it was tried to find out the most favourable slot arrangements and the corresponding suction volumes by means of drag measurements in the wake and of checking measurements of the boundary layer. The slots not used for suction were always pasted over. Only at the beginning of the measurement all the slots were plastered in order to have a completely smooth surface for the comparison measurement on the aerofoil without slots. We saw that the laminar running length could be extended, suction began before transition point. The laminar conditions could thus be kept along more than 90 per cent. of the wing chord. For the best of the combinations which could be taken from the measurements we stated a reduction of resistance of 48 per cent. as against the

aerofoil without slots. The additional power of the blower according to formula (1) still give a saving of 32 per cent. in the coefficient of the propulsive power  $C_{perf}$ . If suction first began behind the beginning of the transition zone, the laminar conditions could no longer be kept in spite of greatest suction.

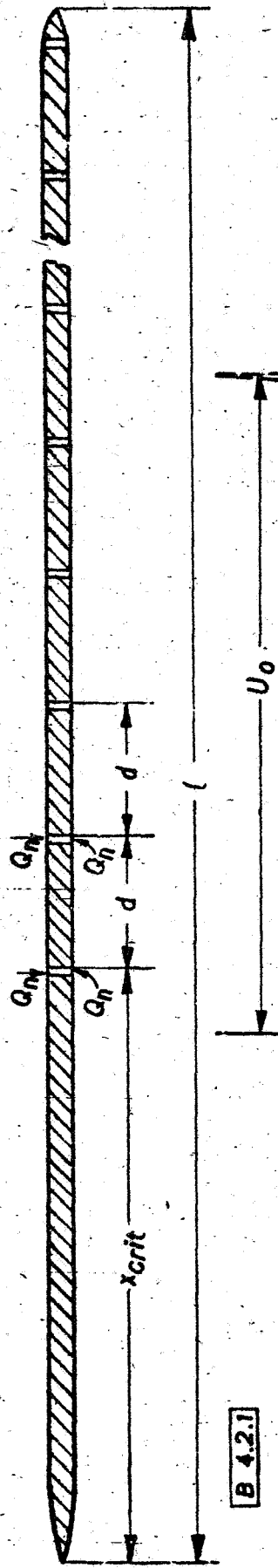
The positive result of this test was followed by a series of theoretical papers on continuous suction of the laminar boundary layer and by corresponding calculations of stability. They will be the subject of section 3.2 of this monograph.

A further suction test was made with a profile NACA/64 [31]. This test aimed, too, at finding out the most favourable combination of the many available suction slots by a try method. The R-number was twice that of the first test, hence  $3.2 \times 10^6$ . With symmetrical incident flow the laminar conditions could also be kept along more than 90 per cent. of the chord, and for suction on both sides we obtained at best a reduction of drag of 60 per cent. of the value for the aerofoil with closed slots. According to the above reflections, considerable savings of propulsive power still existed on the flat plate for the suction of Blasius' profile as far as a velocity of 85 per cent. of the potential velocity (compare Fig.6), whereas a further suction seemed to be nugatory, since it did not cause any extension of the laminar running length. This, however, needs not be contradictory to the test result just mentioned; for, on the one hand, the power conditions for the flat plate are more favourable than for the aerofoil, with the latter the pressure coefficient  $C_p$  in Eq.(1), but assumes a finite negative value varying according to the position of the suction slot. On the other hand the sink effect was not taken into consideration in the case of the flat plate. Such an effect, however, exists for strong suction and influences the development of the boundary layer behind the suction slot by means of its pressure field in a favourable way; thus an extension of the laminar running length will result from the increase of suction beyond the limit of 85 per cent. This extension, of course, is not profitable, since it requires too great suction volumes. This case was probably given for one or more of the 6 suction slots which are open in the measured optimum combination. Supposing this we find the above-mentioned facts to be confirmed that in all cases with considerable savings of propulsive power the suction have to be so small that we need not take into consideration the sink

effect. Moreover the tests showed that in the measured optimum case the laminar conditions were no longer kept when increasing the R-number beyond  $3.2 \times 10^6$  even if the suction volumes through the open slots were increased to the utmost. Hence we see that the sink effect, if supposed to take part in keeping the laminar conditions is only small and that the above discussed test was actually carried out near one of the power peaks (being infinitely high in reality) of the curves in Fig.6.

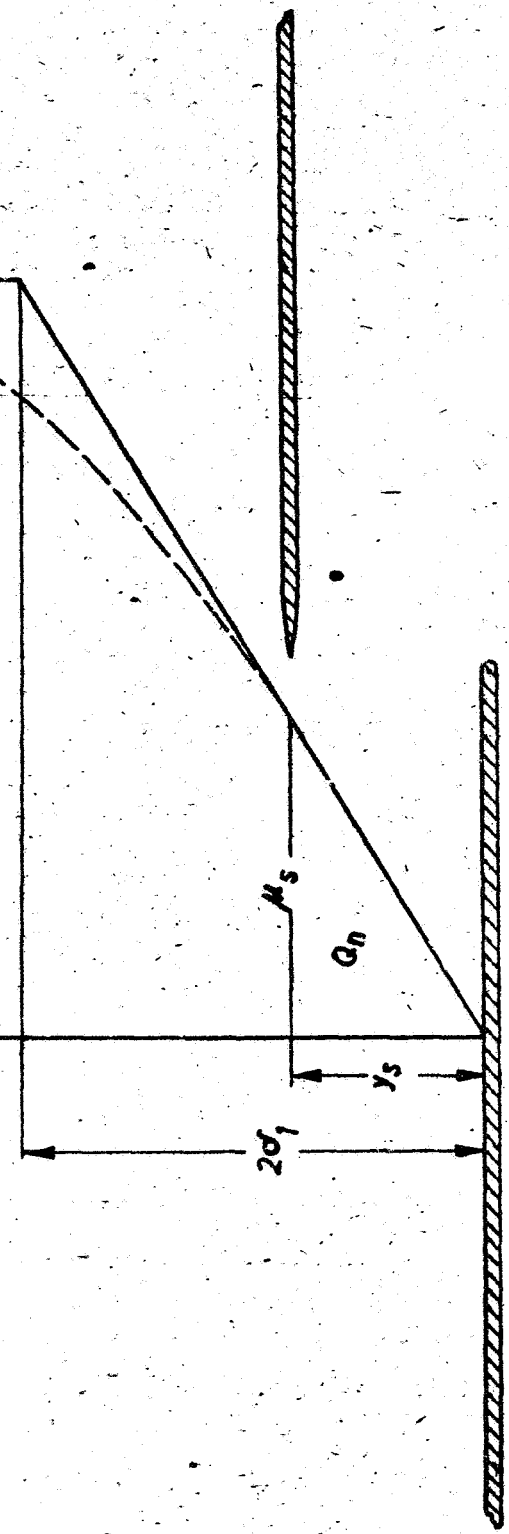
According to these explanations it is clear in what direction we can find improvements of this test results: The distance between the slots must be reduced so far by multiplying the number of slots that it is beyond the above mentioned performance peaks of Fig.6.

The idea suggests itself to avoid the occurring technical difficulties by choosing no longitudinal slots along the span but by choosing sufficiently perforated surfaces. The latter method was applied in a third suction test which was made on a perforated flat plate [33]. The holes had a size of 10 mm in spanwise direction and of 2 mm in chordwise direction. Their distance in flow direction amounted to 4 mm. These measurements were also unsuccessful. The laminar conditions could only be kept by relatively great suction volumes so that no savings of propulsive power resulted. We suppose that the sharp edges of the slots involve disturbing effects which act as far as the stagnation point arising there by suction is located downstream the rear edge of the slot; for only then both slot edges are not in the outer flow of the suction material. Then the sharp edges do not longer cause disturbances of the outer flow. This would first be the case for the chosen kind of perforation for suction volumes which are by far too great in order to allow savings of propulsive power as compared with the non-perforated flat plate. There are obviously two possibilities to improve this arrangement; either the sharp edges of the slots are avoided by suitable punched holes or the widths of the slots are essentially reduced so that the total suction volume remains small, though the suction through a single slot is so great that the just discussed favourable backward position of the stagnation point is obtained for each slot.



[B 4.2.1]

Fig.1: Notations on a flat plate in parallel flow with suction for keeping the boundary layer laminar.



[B 4.2.2]

Fig.2: Notations on an overlapped suction slot when the "triangular profile" is taken as basis for the laminar boundary layer.



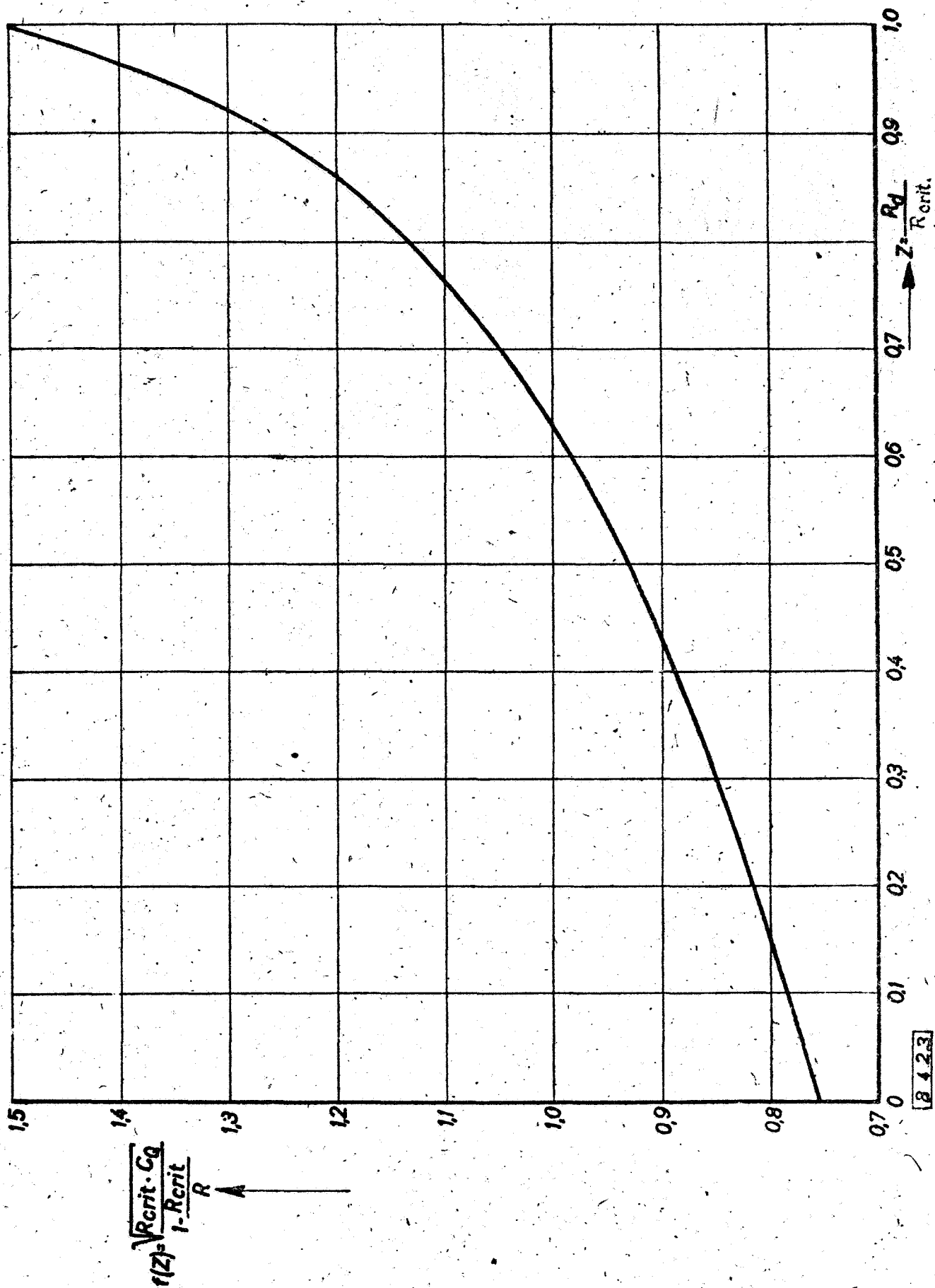


Fig. 2: Representation of the approximate formula (16) for the calculation of the suction of the laminar boundary layer on a flat plate in parallel flow.

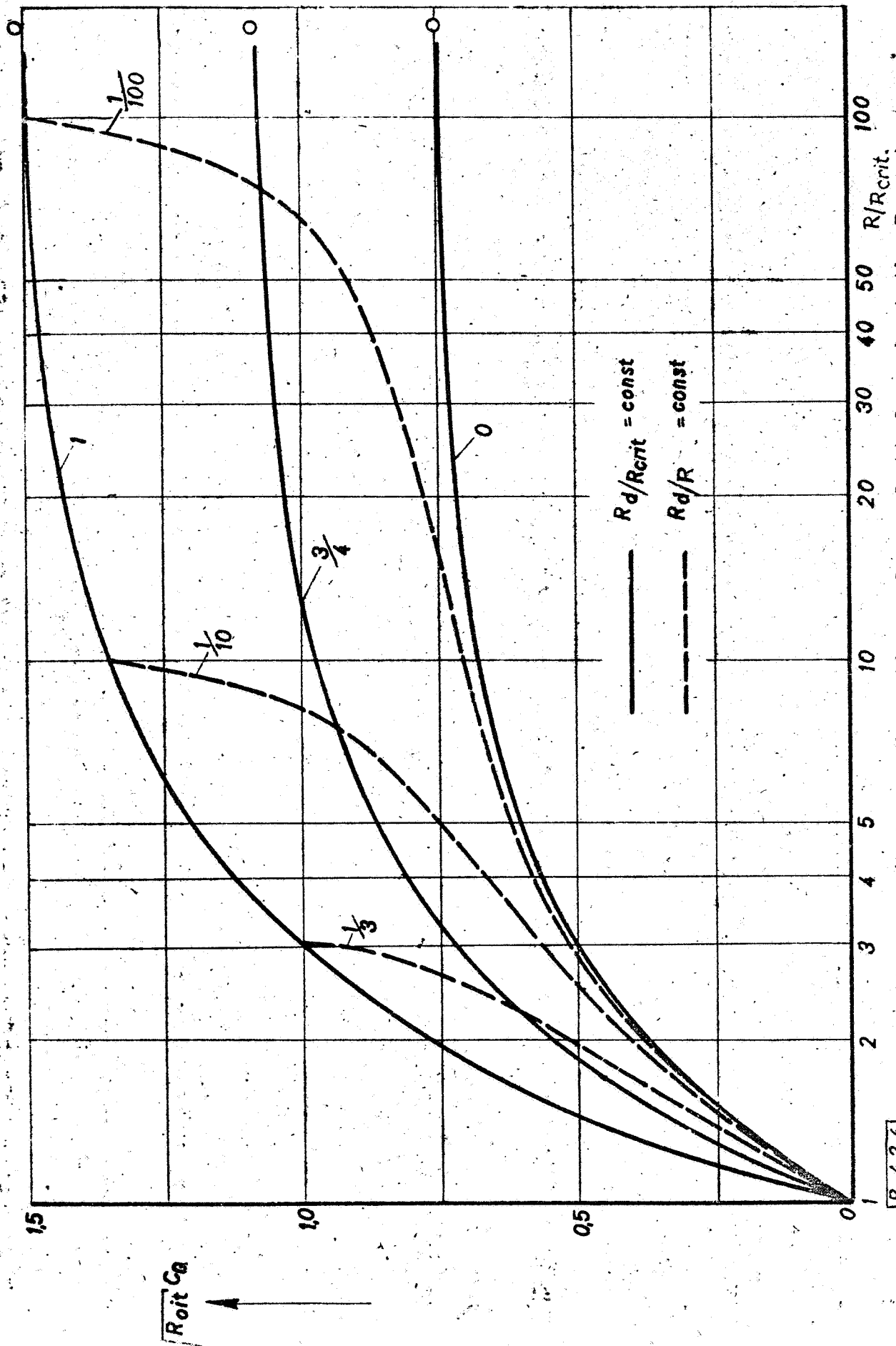


Fig. 4: The coefficient of suction volume plotted against the R-number for various values of the parameters  $R_0/R_{crit}$  and  $R_0/R$  in the case of the flat plate in parallel flow.

B 4.2.4

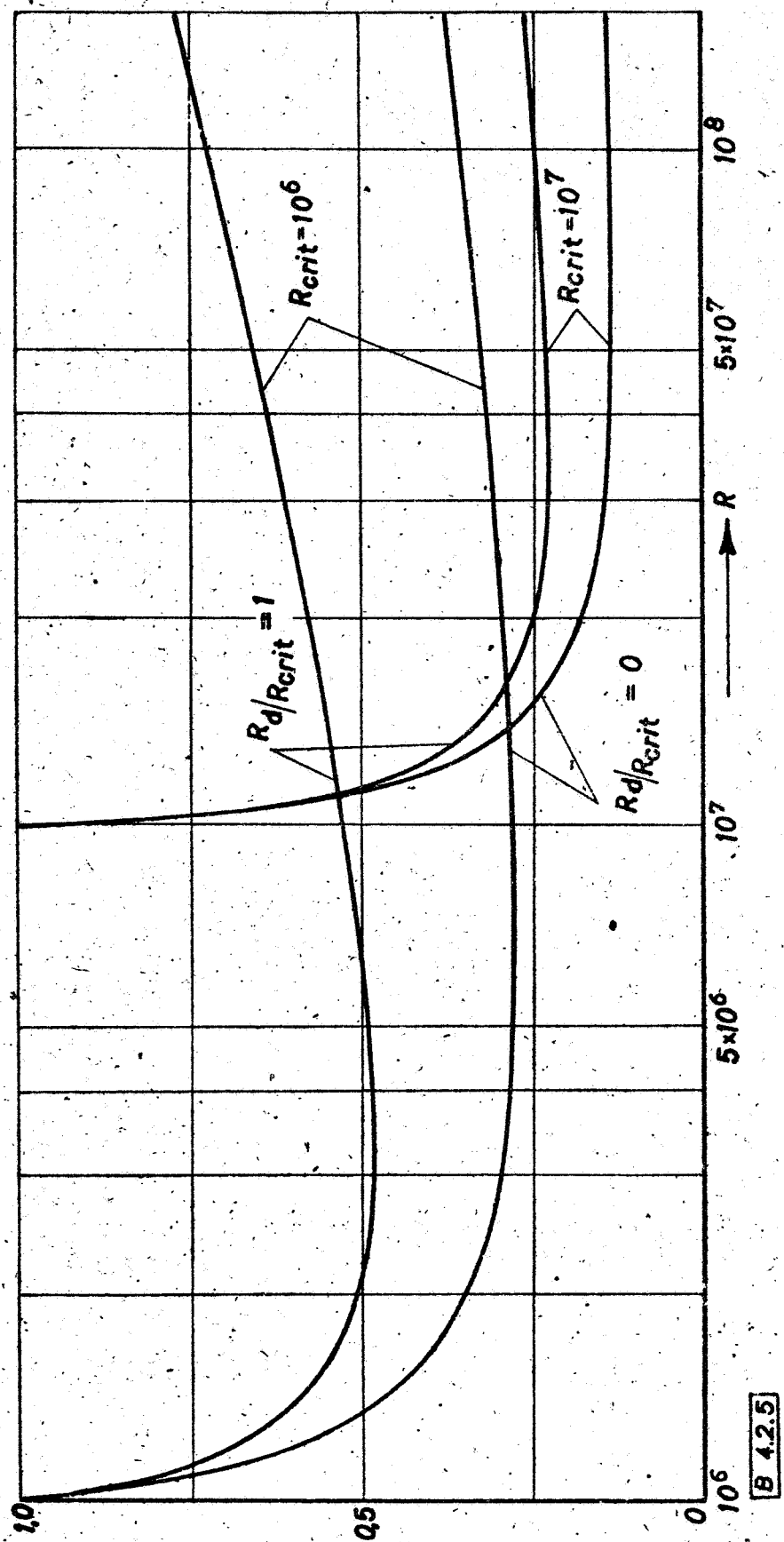
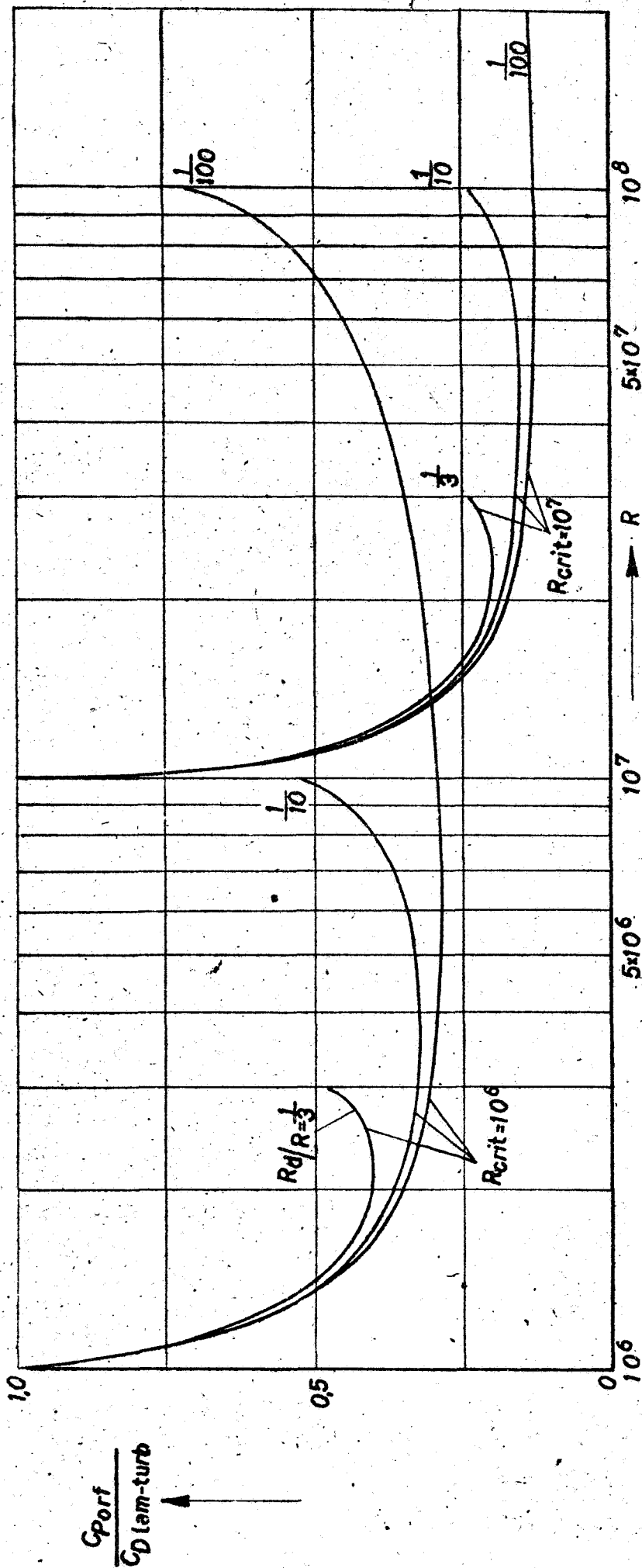


Fig. 5: Diagram for calculating the savings of propulsive power when the laminar conditions are kept by suction of the flat plate in parallel flow, the parameter  $R_d/R_{crit}$  being kept constant.

B 4.2.5



B 4.2.6

**Fig. 6:** Diagram for calculating the savings of propulsive power when the laminar conditions are kept by suction on the flat plate in parallel flow, the parameter  $R_d/R$  being kept constant.

### 4.3 Influence of Surface Conditions on the Transition Point.

By H. Holstein.

#### 4.31 General Requirements for Similitude in the Case of Bodies with Surfaces which are not Smooth everywhere.

If there is geometrical similitude between two bodies in flow the surfaces of which are perfectly smooth everywhere the condition that

$$R = \frac{U \cdot l}{\nu} \quad (1)$$

has the same value in both cases suffices for guaranteeing aerodynamical similitude.  $U_0$  is the velocity of the incident flow,  $l$  is a suitable length and  $\nu$  is the kinematic viscosity. If the surfaces of the two bodies in question, however, are no longer perfectly smooth everywhere, we can define a length  $k$ , which is vertical to the surface and denotes the maximum of the mean level of disturbance. Then the geometrical relation

$$\left(\frac{k}{\delta_1}\right)_1 = \left(\frac{k}{\delta_1}\right)_2 \quad (2)$$

will still be required at least for aerodynamic similitude,  $\delta_1$  is the thickness of displacement.

In the case of model test it will always be possible to satisfy the condition (2); for we have only to choose a suitable grain size. The condition (1), however, will generally not be satisfied, since either the dimensions of the model or the velocities of the incident flow do not reach the corresponding values of the full scale construction. With model measurements we shall be generally interested in having the transition point of the laminar boundary layer at the same point as in the case of the full scale construction; for only then statements on the drag can be transferred from the model measurement to the full scale construction. In order to obtain this similitude with respect to the position of the transition point, we have to compensate the stabilizing effect of a too small  $R$ -number formed according to formula (1) by increasing the relative level of disturbances  $k/\delta_1$ . Eq. (2) has to be changed in a suitable way into the inequality

$$\left(\frac{k}{\delta_1}\right)_{\text{model}} \geq \left(\frac{k}{\delta_1}\right)_{\text{full scale construction}} \quad (3)$$

When forming R-numbers by means of the length in (3) and of the velocity of the incident flow  $U_0$  and the kinematic viscosity  $\nu$  and considering

$$\frac{U_0 \cdot \delta_1}{\nu} = \text{const.} \quad \sqrt{\frac{U_0 \cdot l}{\nu}} = \text{const.} \cdot \sqrt{R}$$

according to Prandtl's equation of the boundary layer we can write (3) in the form

$$\left( \frac{R_k}{\sqrt{R}} \right)_{\text{model}} \geq \left( \frac{R_k}{\sqrt{R}} \right)_{\text{full scale construction}} \quad (4)$$

where equality only holds when the model and the full scale construction have the same size. On the other hand the left-hand side has to be chosen the greater as against the right hand side, the smaller the model as compared with the full scale construction.

When the model has to be investigated at reduced velocity formula (4) with fixed grain size  $k$  requires that the chord of the model has still to be reduced more considerably than the velocity. This is obviously quite contrary to the requirements to be satisfied when using models with perfectly smooth surfaces (compare formula (1)). Whether the model test is to be based on formula (1) or formula (4) in a given case will, according to the above statements, depend on whether considerable displacements of the transition point will be expected when passing from the model test to the full scale construction. If so, formula (4) will be preferred owing to the great influence of the position of the transition point on the resistance. In this case, for instance, model tests on the influence of spray varnish of different roughnesses (camouflage paints), which are meant to be used for the full scale construction, cannot be transferred to reality if they were made with about the same model sizes but at reduced velocities [40; 47]. The same obviously holds for original aerofoils [44; 45; 46] in the wind-tunnel. Here the sign of inequality of formula (4) would even have to be written in the inverse sense. In this case  $k$  and  $l$  are equal for the model and the full scale construction, hence only  $\sqrt{U_0}$  remains on both sides of (4). All measurements, however, remain reasonable if the transition point on the model is displaced forward so far that no remarkable further forward motion can take place when passing to the full scale construction; for the influence of roughness on the turbulent boundary layer is known to depend only very slightly on the R-number.

In wind-tunnels, of course, the degree of flow turbulence influences the position of the transition point, too, and it would be possible in principle to compensate the influence of a too small level of disturbance  $k$  by a corresponding turbulence of the wind-tunnel flow. The present state of knowledge is not sufficient for the application of this method. If we know the position of the transition point for the full scale construction, the corresponding position of the transition point for the model can also be obtained artificially by means of a sufficiently great disturbing wire in the case of a model with too favourable surface conditions. Details will be given in one of the following sections.

#### 4.32 Theoretical Propositions for the Determination of the Critical Level of Disturbance.

Beyond the indication of an inequality we look for quantitative theoretical statements on the influence of surface disturbances on the position of the transition point. Here an hypothesis on the critical level of disturbance cannot be dispensed with. Such an hypothesis was put <sup>up</sup> by S c h i l l e r [34] : With respect to its configuration of streamlines a sufficiently viscous flow is known to behave similar to a potential flow though not quantitatively but in so far as the streamlines follow the contour of the body everywhere without separations, whatever may be the shape of the body. Only at a certain number

$$\frac{U_o \cdot d}{\nu}$$

where  $d$  is a length taken from the frontal area of the body, considerable vortices begin to form. When increasing this R-number further on they begin to detach and form a street of disturbances behind the body. The corresponding process takes place in a small scale for bodies with disturbances on the surfaces- and this is the contents of Schiller's hypothesis. Similarly the critical R-number

$$R_{u_k} = \frac{u_k \cdot k}{\nu} \quad (5)$$

is then characteristic in this case with a given level of disturbance  $k$ .  $u_k$  is proportional to the velocity in the boundary layer at the distance  $k$  from the wall immediately before the point of disturbance.

G o l d s t e i n [37] investigated the relation

$$R_k^* = \frac{v^* \cdot k}{\nu} = \sqrt{\frac{u_k \cdot k}{\nu}} \quad (6)$$

in detail, where

$$v^* = \sqrt{\frac{\tau_0}{\rho}}$$

means the so-called "velocity of the skin friction". As is easily seen, the relation (6) holds identically as far as  $u_k$  is still in the linear part of the laminar boundary layer profile. He found that (6) too, holds, with good approximation for distances  $k$  from the wall outside the linear part, since the terms of correction first are very small. We are therefore allowed to follow Schiller's hypothesis and to choose the value  $R_k^*$  to be calculated more conveniently instead of  $R_{uk}$  as critical R-number for surface disturbances. In order to calculate the velocity of the skin friction  $v^*$  at any point of the body we can for instance make use of the well-known calculating method for laminar boundary layers according to Pohlhausen. Thus according to T a n i [39] Schiller's hypothesis yields the explicit formula

$$\frac{k}{l} = \frac{R_k^*}{A} \cdot R^{-0.75} \quad (7)$$

with

$$A(s) = \sqrt{\left(2 + \frac{\lambda}{6}\right) \cdot U \cdot \sqrt{\frac{dU/ds}{\lambda}}} \quad (8)$$

The expression  $A$  has been introduced, since it does not depend on the R-number but on the contour of the body only. Here  $\lambda$  is the well-known shape parameter of the laminar boundary layer according to Pohlhausen,  $U$  the local velocity, and  $s$  the evolution along the contour beginning at the stagnation point. These quantities are made non-dimensional by the velocity of the incident flow or a suitable length, respectively.

If we enlarge the left-hand side of (7) to  $R_k/R$  and multiply Eq. (7) by  $\sqrt{R}$ , we obtain

$$\frac{R_k}{\sqrt{R}} = \frac{R_k^*}{A} \cdot R^{-0.25} \quad (9)$$



Since the first factor on the right-hand side is constant for a given point of the test body according to Schiller and Tani, the left-hand side Eq.(9) decreases with increasing  $R$ . Comparing (9) with the inequality (4) which holds without limitation, we see that the two relations are in good accordance. If the transition points on the model and on the full scale construction correspond to each other the level of disturbance  $k$  to be chosen for a model test will be taken now from the equation

$$\left(\frac{R_k}{\sqrt{R}}\right)_{\text{model}} = \left(\frac{R_k}{\sqrt{R}}\right)_{\text{full scale construction}} \quad (10)$$

which results from (7) or (9), instead of from the inequality (4); (the degree of turbulence is assumed to be zero).

The quantity  $A$  is given by (8) is a measure of local sensitivity of the behaviour of the laminar boundary layer to surface disturbances; for according to (7) the admissible level of disturbance  $k$  is greater, the smaller  $A$  in Fig.1 shows the curve of  $A(s)$  for two examples, viz. for the flat plate and for an elliptical cylinder of the thickness ratio 1:3 in a flow parallel to its greater axis. The latter was chosen, since the calculation according to Pohlhausen was already available for it [36]. This calculation had only to be somewhat completed near the stagnation point. The abscissa is referred to half the circumference in the case of the cylinder and so the chord in the case of the plate. The calculation of  $A$  for the flat plate cannot be simply made according to (8) owing to the indeterminate expression ( $\lambda = 0$ ,  $dU/ds = 0$ ) in (8). The direct calculation by means of Blasius' formula gives

$$R_k^* = 0.576 \cdot R_k \cdot R_x^{-0.25} \quad (11)$$

(valid for the flat plate).

Comparing (7) with (11) we obtain

$$A = \frac{0.576}{\sqrt{x/l}} \quad (12)$$

(valid for the flat plate).

As is seen, the behaviour of  $A$  in both cases of Fig.1 is quite different for small values of  $s$ : whereas the  $A$ -curve for the flat plate shows an unlimited rise for  $s \rightarrow 0$ ,  $A$  reaches a maximum value at about  $s = 0.05$  for the elliptical cylinder, then it drops to zero for  $s \rightarrow 0$  - obviously due to the stagnation point. We can obviously generalize this result obtained for the elliptical cylinder

by saying: Any body with a stagnation point in front has a point of greatest sensitivity to disturbances of the laminar boundary layer on its upper as well as on its lower side. The sensitivity chiefly decreases upstream this point due to the decrease of the potential velocity towards the stagnation point and downstream that point it decreases due to the increase of the boundary layer thickness. As is seen from the velocity distribution  $U(s)$  given in Fig.1, the maximum sensitivity does not coincide with the maximum velocity, but is reached much earlier. As we can learn from the comparison with the limiting case of the flat plate, the maximum sensitivity assumes higher and higher values and moves towards smaller abscissae the smaller the thickness.

The measure of sensitivity  $A$  can be determined numerically in any case with given pressure distribution of the test body, whereas the second value  $R_k^*$  required according to Eq.(7) for the calculation of the admissible level of disturbance, has to be determined by experiments.

#### 4.33 Tests on Bodies with Surface Disturbances.

##### 4.331 Tests with Single Disturbances.

T a n i [39] has carried out tests on a flat plate with three disturbing wires of different thicknesses. He forms the mean value

$$R_k^* = 13$$

from his results of measurement. Let us give details of Tani's measuring method. This instrument for measuring the transition point, a Pitot tube near the wall, was arranged at a fixed distance (700 mm) from the leading edge of the plate. A disturbing wire transverse to the direction of flow along the surface of the plate was subsequently arranged at different points in front of the Pitot tube. The velocity of the incident flow was then increased in each case as far as the total-pressure rise characterizing the transition was indicated by the Pitot tube.

This experimental method only gives sufficient particulars of the behaviour of the laminar boundary layer as against surface disturbances if the transition point keeps its position for too small a disturbance but advances suddenly to the disturbing point, when the efficient level of disturbance is reached. If the transition point, however, moved gradually and continuously from its

original position towards the leading edge of the plate when tending to approach the critical disturbance value, T a n i ' s measurements would be incomplete: For in this case the numerical value  $R_k^* = 13$  obtained by him holds only for the arbitrary position of the instrument for measuring the transition point and would vary with the position of the instrument. The latter fact really seems to prove right according to measurements made by S c h e r b a r t h [42]. Scherbarth used a fixed distance (500 mm) of the disturbing bodies from the leading edge of the plate and determined the position of the transition point for different velocities of the incident flow by means of a sliding Pitot tube. He used sheet metal strips 20 mm in width as disturbing bodies instead of wires. This fact will hardly influence the results.

To compare T a n i ' s and S c h e r b a r t h ' s results of measurement we calculate by interpolation those levels of disturbances  $k$  from Scherbarth's curves for which the transition takes place at a distance of 700 mm from the leading edge of the plate (i.e. the location of Tani's measurements of the transition point). Doing so and plotting the associated  $R_k^*$ -values against the level of disturbance  $k$ , we obtain Fig.2. Hence the result is no constant value for  $R_k^*$  but a curve which decreases with the level of disturbance  $k$ . The way, however, in which S c h e r b a r t h measured the level of disturbance of the sheet metal strips is not known. We can conclude with some certainty from the smooth numerical values for  $k$  that he has simply taken the thicknesses of the sheet metal strips as levels of disturbances. In reality, glues and irregularities of the strips surfaces will have caused a considerable increase of the effective level of disturbance, especially with thinner strips. In this case the measuring points (Fig.2) which are too low would rise along a vector drawn from the origin so that the hypothesis  $R_k^* = \text{const.}$  would still be justified. There is another explanation of the decrease of  $R_k^*$  with  $k$ : The value of  $R_k^*$  has only the character of a limit of stability above which the transition takes place after running through a more or less long zone of excitation. For reasons of similitude the zone of excitation would then be shorter for small levels of disturbance than for great ones. In order to mark the limit of stability the points (Fig.2) associated to small levels of disturbance  $k$  had to move downwards a little whereas those associated to greater levels of disturbance  $k$  had to move downwards a correspondingly greater distance so that the hy-

pothesis  $R_k = \text{const.}$  would be justified, too. The final decision, however, must be reserved to exacter measurements.

Measurements of the transition point on disturbing wires were also made for aerofoils. Tani [39] obtained the value  $R_k^* = 13$  for a symmetrical laminar profile. His measuring method corresponded to that described for the flat plate. German measurements [2] made according to the same method gave values of  $R_k^*$  between 9 and 14, on an average 11. The measurements also confirmed the existence of a sensitivity curve as shown in Fig.1; the disturbing wire showed zones in the forward and in the rear part of the aerofoil profiles in which it did not yet disturb the laminar boundary layer in the case of the applied velocity of the incident flow. Tani's measurement did not cover profile zones sufficiently far in front in order to confirm similar conditions. The German measurements with disturbing wires [7; 48] are no measurements of transition points but drag measurements. From all of them results the familiar fact that the drag increase is particular great when the disturbing wires are so far in front on the profile that they do not only cause an increase of the turbulent drag component but they cause a forward displacement of the transition point, too. Knowledges surpassing the familiar facts on the sensitivity of the laminar boundary layer cannot be obtained from them thus they need not be taken into consideration here.

Besides the disturbing bodies in two-dimensional flow discussed so far, the lateral extension of a point disturbance was investigated, too [41; 42]. From the measurements on a flat plate resulted a wedge-shaped region of disturbance behind the point of an aperture angle of about 14 to 18 degrees. With increasing R-number there is a slight increase of this angle. Let us also mention the following phenomenon frequently on wind-tunnel models which have been exposed to the airstream for a considerable time: The rear turbulent part of the test body characterized by an irregular deposition of dust in zigzag, is evidently limited against the forward laminar part. Zigzag figures have the above indicated aperture angle. They are caused by small disturbances incidentally existing on the surface. The turbulence within the regions of disturbance only makes the deposition of dust possible in the airstream. Thus we obtain a good survey of the positions of the transition points on the whole model surface.

We have so far discussed the influence of disturbing bodies with finite level of disturbance  $k$  on the laminar boundary layer. But even in cases where a level of disturbance  $k$  does not exist a given point can disturb the laminar boundary layer, viz. when the surface shows here a discontinuity in curvature. In this case the disturbance is due to the particularities of the pressure distribution occurring at a discontinuity in curvature. The potential theoretical investigation of such an irregularities showed [43] that the velocity distribution on the wall has here a point of inflection with a tangent normal to this wall and consequently this velocity distribution still shows fluctuations near such a point, too. These fluctuations fade away rather slowly with increasing wall distance, so that a disturbing influence on the laminar boundary layer is still possible in spite of the finite thickness of displacements. Measurements on the laminar profile confirmed the fact [1] that a transition can be involved by a discontinuity in curvature contour used was a circular biangle with a thickness ratio 0.1. In order to obtain a rounding of the nose, the leading edge of the circular biangle had been cut off and replaced by a small circular arc. Thus a discontinuity in curvature arose at the joint, viz. the radius of curvature referred to the chord suddenly varied from 0.01 to 2.6. In curve (b) of Fig.3 the drag coefficient is plotted against the lift coefficient as it resulted from the measurement on this profile. As is seen, the transition points on both sides are located in front in the case of symmetrical flow. Only with a certain incidence the transition point moves backwards on the pressure side and will thus produce a decrease of the drag coefficient. This behaviour concluded from the drag curve could be confirmed by measurements of the transition points. Only a sufficiently great positive pressure gradient will consequently counterbalance the disturbance due to the discontinuity in curvature. Curve (a) is associated to a profile formed by the same circular arcs, only the nose radius is altered to  $1/10$  of that of the above profile. The discontinuity in curvature is consequently 10 times the value of the profile of curve (b). It is located, however, within the range of the strong pressure drop due to the vicinity of the stagnation point. Thus the disturbance cannot become effective in this case either. By the way, high subpressure peaks naturally occur at once on this sharp-nosed profile even with small incidence. Thus the transition point quickly moves forwards on the corresponding suction side. Curve (c) finally shows the drag curve for

the same circular biangle, apart from the nose which is here a parabolic arc so that the curvature of the contour remains continuous. This profile shows the usual behaviour of laminar profiles as described in detail in section 4.1 .

#### 4.332 Tests with Throughout Rough Surfaces.

We have so far discussed single disturbances of the laminar boundary layer. The influence of rough surfaces remains to be investigated, namely surfaces with levels of disturbances statistically distributed. The level of disturbance  $k$ , therefore, can be considered here as statistic mean value only. We can learn from former measurements [35] on flows through tubes which were made rough by means of depositions of sand of different grain size that the influence of such a roughness on the laminar boundary layer will be unimportant in any case with small pressure gradients: neither the thickness of the laminar boundary layer nor its transition point seem to be considerably altered as compared with the conditions of the smooth tube. A recent measurement [49] concerning the influence of roughness on the laminar boundary layer was made on a flat plate the surface of which was subsequently pasted over with sand paper of different roughnesses. Fig. 4 was obtained from the measurements of the transition point  $\delta_{1crit.}$  is the critical thickness of displacement calculated from the measured position of the transition point and from Blasius' formula valid for the smooth plate. The abscissa is referred to the critical thickness of displacement on the smooth plate, since the latter did not prove as constant but as a function of the R-number. When representing the distribution of the measuring points by an average curve the points on the right side of the figure must not be taken into consideration, since those points say that the transition on the smooth plate partly occurred earlier than on the rough plate. This is explained by the fact that partly a waviness of the smooth plate favouring the transition was removed by pasting over the roughness layer, partly an angle of incidence was included with a pressure distribution favourable for keeping the laminar conditions on the rough side. In any case, the small influence of small roughnesses on the transition point is confirmed. A remarkable influence seems to occur only with greater roughnesses of the order of the thickness of displacement, and it will be desirable to clear this by further measurements.

References for 4.1:

- [1] H.Doetsch, Some profile investigations in the Range of small  $C_a$ -values.  
LGL 117 (1939) p.25.
- [2] H.Holstein/  
A.Doneis, Measurements on a laminar profile with extreme backward position of the pressure minimum.  
FB 1522 (1941). 1115.5  
776
- [3] H.Schlichting/  
K.Bussmann, Measurements on laminar profiles. 1115.5  
LGL 149 (1942). Nov 2/43
- [4] H.Holstein/  
A.Doneis, Measurements on four laminar profiles of different camber which were developed from the ellipse.  
FB 1617 (1942). 1115.5  
312
- [5] H.Doetsch, Profile investigations in the 5 x 7 m wind-tunnel of the DVL.  
FB 1621 (1942). 1115.5
- [6] W.Puffert, Three component measurements on swept-back aerofoils and on a whole model with swept-back aerofoils.  
FB 1726 (1942).
- [7] K.Bussmann, Experimental and theoretical investigations on laminar profiles.  
FB 1709/1 (1942).
- [8] H.Doetsch, Tests on the aerofoil profile of the North-American Mustang.  
FB 1712/1 and FB 1712/2 (1943).
- [9] K.Bussmann, Measurement on the laminar profile P-51 Mustang.  
FB 1724 (1943).
- [10] H.Holstein, Measurements on four laminar profiles with different camber which were developed from the ellipse.  
FB 1617/2 (1943). 1115.5
- [11] H.Doetsch, Tests on a laminar profile.  
Techn.Ber.Vol.10 (1943) p.186.
- [12] E.v.Lössl, Reduction of the profile drag by artificial pressure rise in the transition zone.  
Techn.Ber.Vol.10 (1934) p.211.
- [13] E.v.Lössl, Reduction of the profile drag on a symmetrical aerofoil profile by pressure rise in the transition zone.  
Techn.Ber.Vol.10 (1943) p.367.
- [14] S.Weiss, Survey on the German wind-tunnels.  
UM 750 (1943).

- [15] F.Riegels, Russian laminar profiles.  
UM 3040 (1943).
- [16] F.Riegels/  
J.Liese, Aerodynamic calculation of aerofoil profiles.  
Catalogue of the pressure distributions.  
FB 1884 (1943).
- [17] F.Riegels/  
J.Liese, Russian laminar profiles.  
2<sup>nd</sup> Part; theoretical supplements. 1115.5  
UM 3056 (1943).
- [18] Kopfermann/  
Breford, Measurements of the transition point on the  
original aerofoil of the type P 51 Mustang.  
UM 2035 (1943).
- [19] F.Riegels, Russian laminar profiles, 3<sup>rd</sup> Part. Measure-  
ments of the profile 2315 Bis with AVA-nose  
flap. 1115.5  
UM 3067 (1944).
- [20] Kopfermann, Measurements on the Russian laminar profile  
2315 Bis. 1115.5  
UM 2077 (1944).
- [21] H.Doetsch, Report on the special branch "profiles" before  
the special committee wind-tunnels on the 10th  
Nov. 1943 and on the 4th Jan. 1944.  
UM 1190 (1944).
- [22] A.Walz, Measurements on two profiles of 13.6 per cent.  
thickness with small angle of the trailing edge  
in the great tunnel of the AVA.  
UM 3092 (1944).
- [23] Breford/  
Voelz, Measurements on two laminar profiles with high  
R-numbers. 1115.5  
UM 2100 (1944).
- [24] Brennecke, Keeping the boundary layer laminar in the case  
of swept-back aerofoils. 1115.5  
UM 3151 (1944).
- [25] F.Riegels, Russian laminar profiles, Part 4: Drag  
measurements on the profile 2315 Bis. 1115.5  
UM 3159 (1944).
- [26] H.Doetsch, Tests with the Mustang profile on the influence  
of the angle of the trailing edge on the profile  
characteristics. 1115.5  
UM 1488 (1944).
- [27] H.Holstein, Drag measurements on corrugated aerofoils.  
UM 3228 (1945).



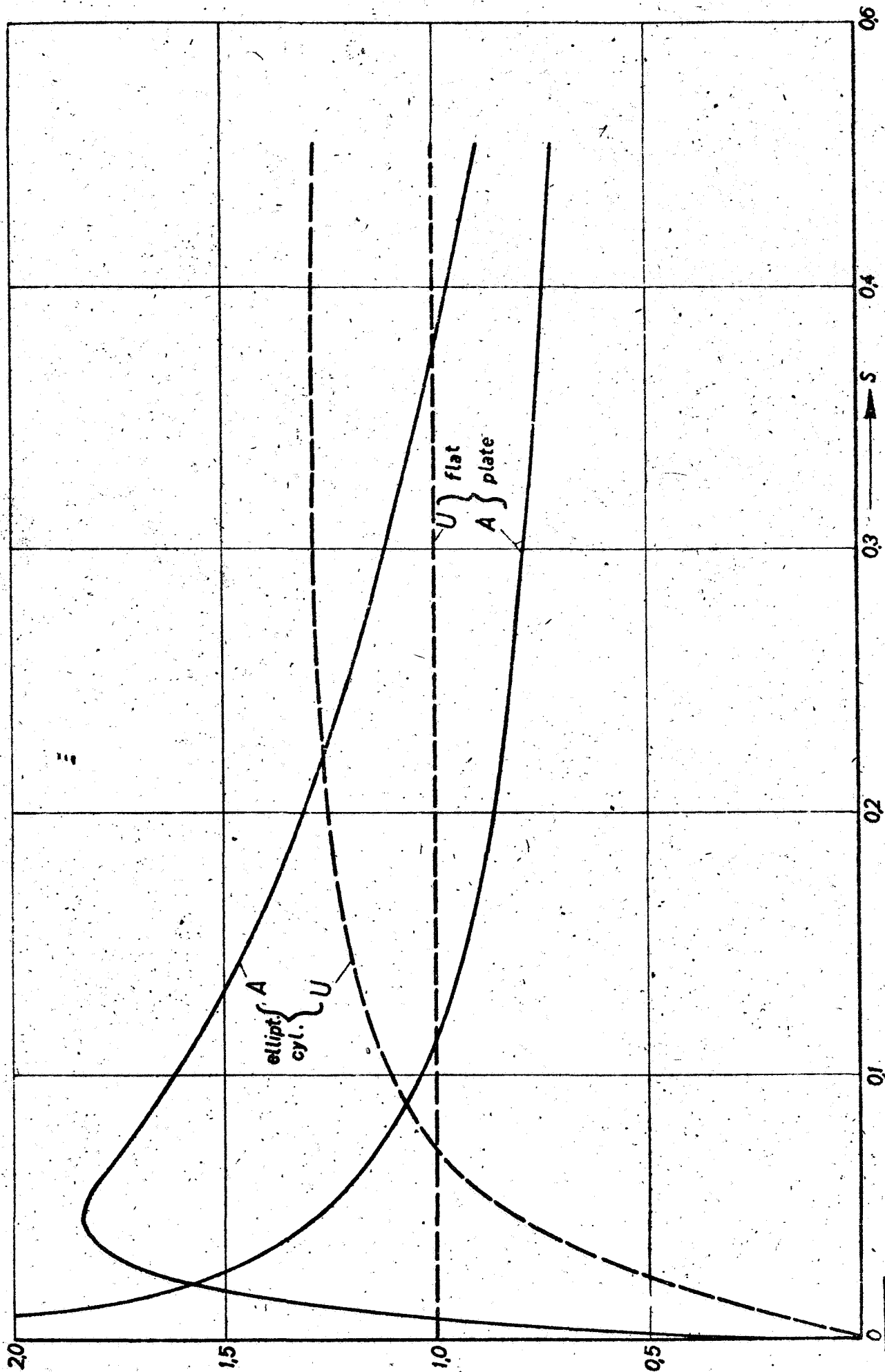
References for 4.2:

- [28] O.Schrenk, Tests with suction aerofoils.  
Lufo 12 (1935) p.10.
- [29] H.Holstein, Aerofoil measurements for keeping the boundary layer laminar.  
LGL S 10 (1940) p.17.
- [30] H.Holstein, The suction of the boundary layer for keeping it laminar, especially on flat plates in parallel flow.  
FB 1542 (1941).
- [31] H.Holstein, Measurements in the case of keeping the boundary layer laminar by means of suction with the profile NA 0012/64.  
FB 1654 (1942).
- [32] H.Holstein/  
A.Doneis, Tests on the regain of pressure by giving the suction slots a suitable shape in the case of suction of laminar boundary layers.  
FB 1773 (1943).
- [33] H.Holstein/  
B.Pekarek, Measurements in the case of keeping the boundary layer laminar by means of suction on a perforated flat plate.  
UM 3222 (1945).

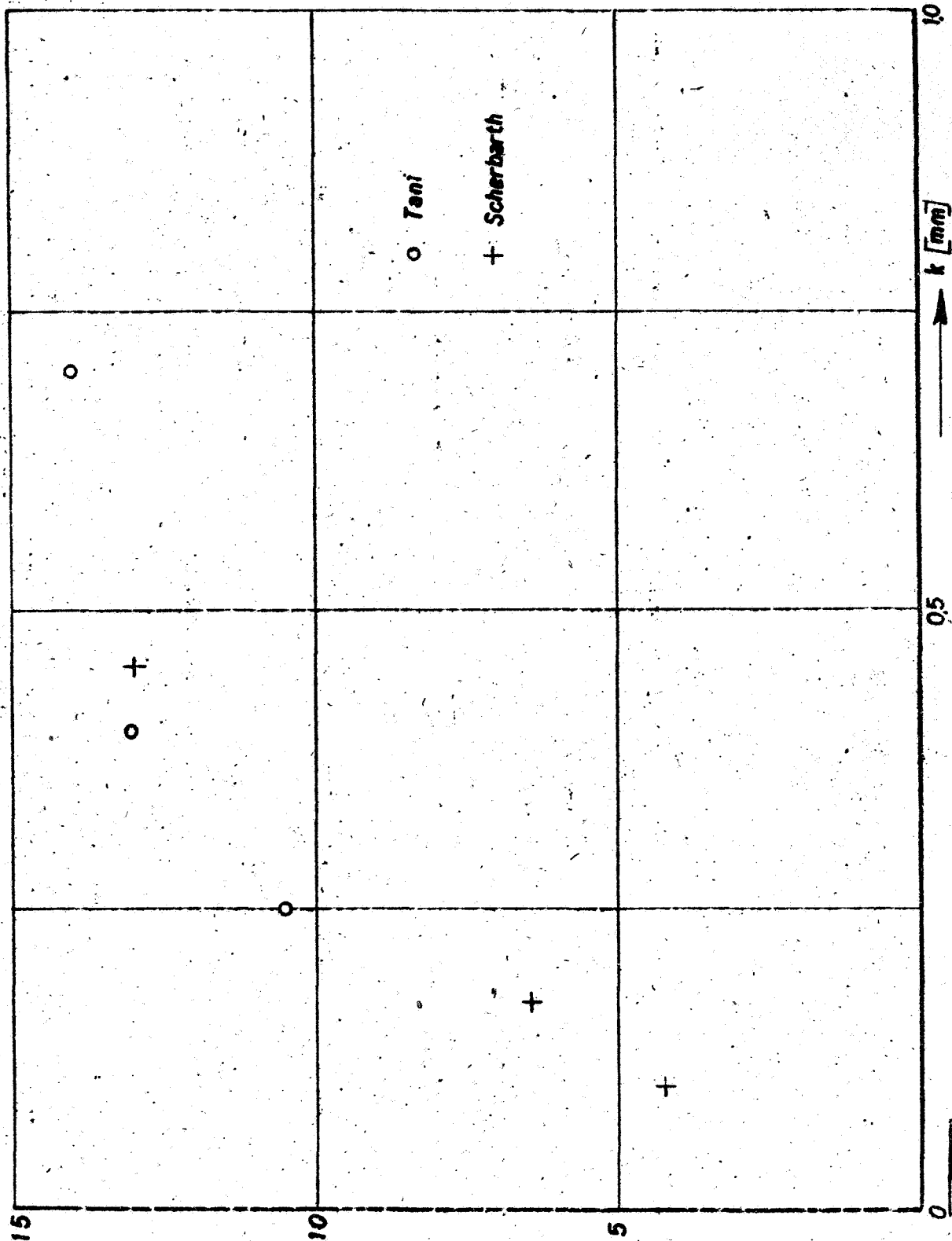
References for 4.3:

- [34] L.Schiller, (Handbook of experimental physics).  
Vol.4, part 4 (1932) p.191.
- [35] T.Nikuradse, Laws of flow in rough tubes.  
VDI-Forschungsheft 361 (1933).
- [36] G.B.Schubauer, Air flow in a separating laminar boundary layer.  
NACA-report 527 (1935).
- [37] S.Goldstein, A note on roughness.  
ARC-Rep. and Mem. 1763 (1937).
- [38] A.D.Young, Surface finish and performance. The antipathetic problems of aerodynamic refinement and practical construction.  
Aircr.Engng.11 (1939)pp.339-341 and 350.
- [39] J.Tani/  
R.Hama/  
S.Mituisi, On the admissible roughness in the laminar boundary layer.  
Ber.Aeron. Forsch.Inst.Kaiserl.Univ.Tokio,  
Vol.15 (1940) p.417.
- [40] P.Kretz, Profile drag measurements on rough surfaces.  
FB 1532 (1941) and Techn.Ber.Vol.8 (1941) p.121.

- [41] Scherbarth, Boundary layer measurements behind a punktiform disturbance in laminar flow.  
FB 1532 (1941) and Jahrb.(1942) d.DL I p.51.
- [42] A.W.Quick, Some remarks on laminar profiles and on the behaviour of the laminar boundary layer under the influence of disturbing bodies.  
LGL 141 (1941), Nachtragsbericht, p.1.
- [43] A.Betz, Velocity distribution of the flow near a wall with discontinuities in curvature.  
Lufo 19 (1942) p.129.
- [44] H.Doetsch, Profile drag measurements on model aerofoils in smooth sheet metal construction produced in series.  
FB 1731 (1943) and Techn.Ber.Vol.10 (1943) p.106.
- [45] Breford/  
Möller, Measurements on the original aerofoil type P-51 "Mustang".  
FB 1724/2 (1943).
- [46] H.Doetsch, Tests on two model aerofoils in sheet metal construction with laminar profiles.  
FB 1855 (1943).
- [47] Runkel, Measurements of the profile drag and of the boundary layers on a NACA 23012 profile with smooth and with rough paint.  
UM 3507 (1943).
- [48] H.Doetsch, On the influence of surface disturbances on the drag of the aerofoil.  
UM 1233 (1944) and LGL 176/1 p.5.
- [49] H.Holstein, Tests with a flat plate in parallel flow concerning the roughness influence on the transition point.  
UM 3110 (1944).



**B 4.3.1** Fig. 1: Resumptive  $A(s)$ -curves representing the sensitivity of the laminar boundary layer to disturbances, as well as velocity curves  $U(s)$  for the flat plate in parallel flow and for an elliptical cylinder.



B 43.2  
Fig. 2

Experimental results of measurements with disturbing wires of different diameter  $k$ . The ordinate is a Re-number formed with the velocity of the skin friction stress at the transition point.

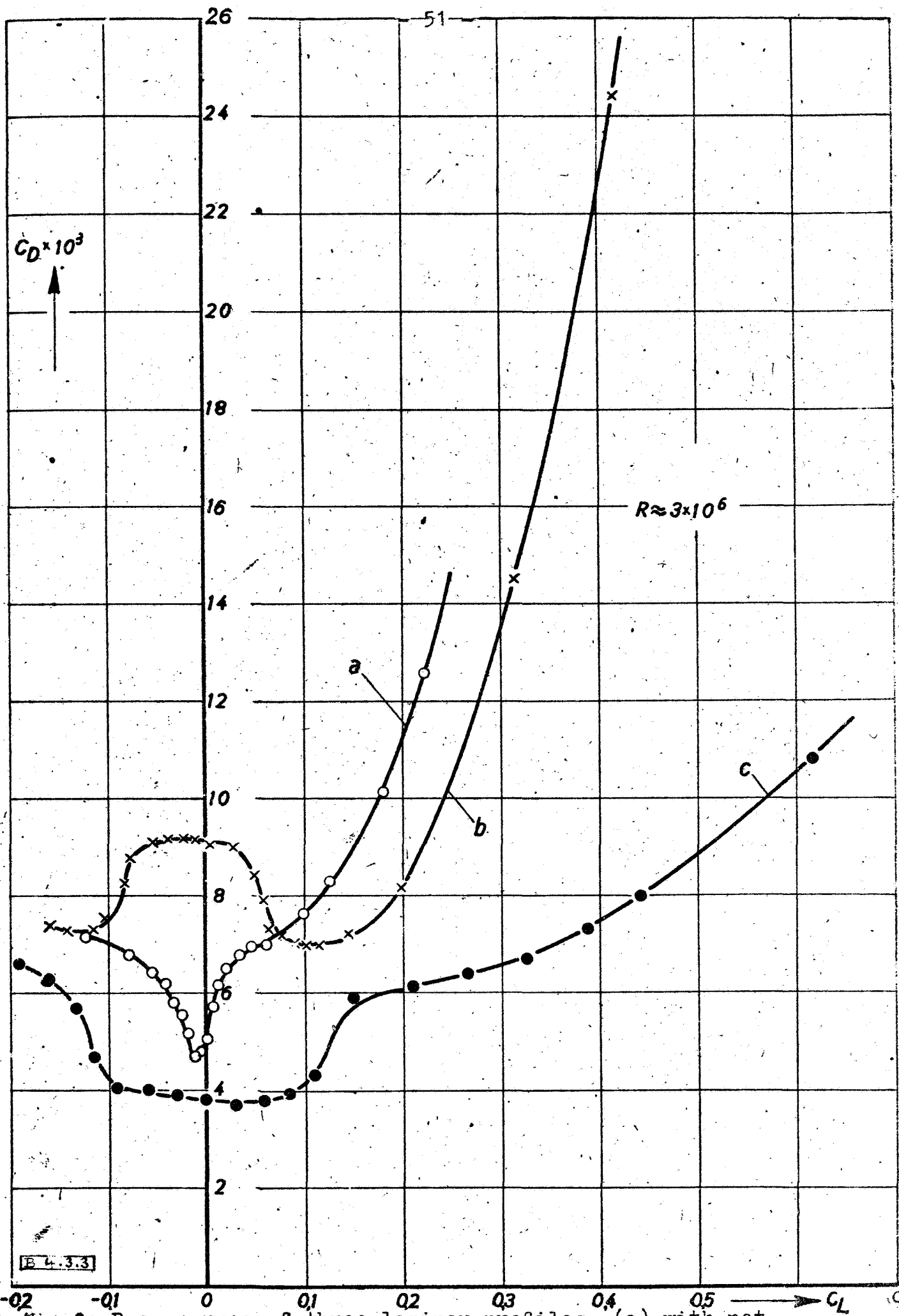
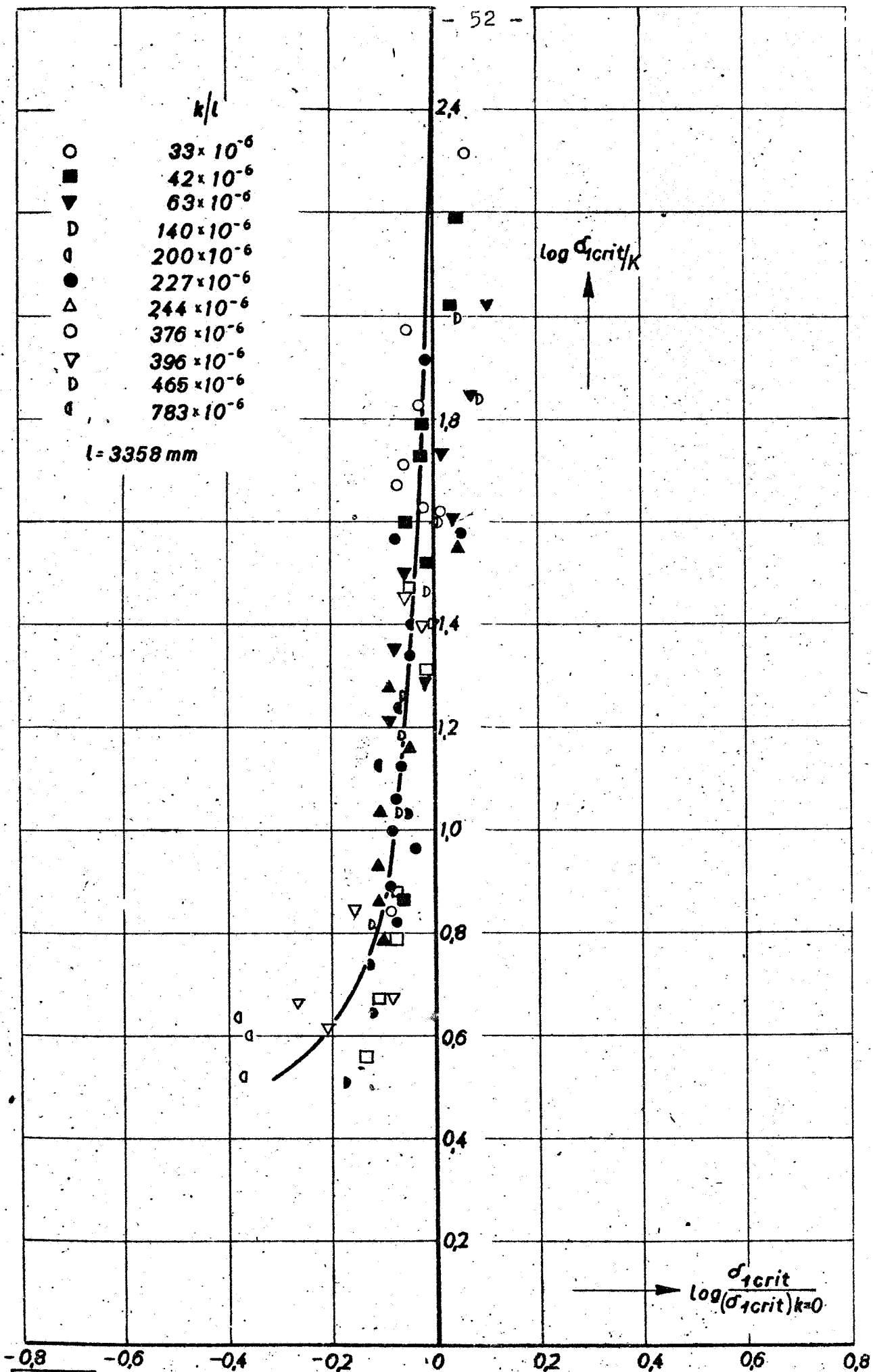


Fig. 3: Drag curves of three laminar profiles, (a) with not disturbing, (b) with disturbing, (c) without discontinuity



B 4.3.4

Fig. 4: Result from measurements of the transition point on a flat plate for different roughnesses.